Modeling Environmental Drivers of Wildlife-Vehicle Collisions in the Methow Valley, Washington to Inform Engineering Solutions

Jeffrey A. Manning
Assistant Professor
jeff.manning@wsu.edu

and

Caren S. Goldberg
Assistant Professor

School of the Environment
Washington State University
P.O. Box 642812
Pullman WA 99164-2812

Final Report
Submitted to:

Washington State Department of Transportation
North Central Region
Office: (509) 667-2876

March 30, 2020

WSDOT Contract No. T1462-15

TABLE OF CONTENTS

EXECUTIVE SUMMARY

The purpose of this study was to provide the Washington State Department of Transportation (WSDOT) with scientific information regarding the patterns of mule deer use, road crossings, and wildlife-vehicle collisions along State Route 20 within north-central Washington's Methow Valley. This work was established under WSDOT's Federal Lands Access Program funded project titled "SR 20/ North Cascades Highway State Route 20 (Forest Service Road #32)."

This report describes the findings from 60 remote game cameras from April through October 2017, visual surveys to locate live deer from May through August 2017, mark-resight surveys for deer carcasses in April and October 2017, radio-tracking of 22 adult female deer January 2018 – August 2018, and 49 UHF data loggers recording radio-tracked deer along State Route 20 January 2018 – October 2018.

This study was funded by WSDOT, under contract T1462-15; all research activities were authorized under Washington State University Institutional Animal Use and Care Committee Animal Subjects Approval Form 04968, Washington Department of Fish and Wildlife (WDFW) Scientific Collecting Permit 17-339, and WDFW Right-of-Entry permit 110381,110366,110309, dated January 22, 2018. Results from this study were presented at regional venues (Appendix C)

April 2016

INTRODUCTION

Wildlife-vehicle collisions constitute a substantial component of mortality in many resident and migratory wildlife populations (Bissonette 2002). With traffic increasing on highways intersecting wildlife habitats across the United States, numbers of wildlife-vehicle collisions continue to rise, causing concern for human safety, financial burdens, and impacts on wildlife populations. Nationally, deer-vehicle accidents result in approximately 200 human fatalities each year and insurance payments of nearly $2 billion annually (Figure 1). Across Washington State, the average number of deer carcasses attributed to deer-vehicle collisions that were removed from highways between 2009 and 2014 exceeded 3,500 per year [Washington State Department of Transportation (WSDOT) unpublished data] compared to 1,200 carcasses per year less than a decade earlier (Myers et al. 2008). Mule deer-vehicle collisions along portions of numerous state and federal highways have been routinely documented in eastern Washington (Myers et al. 2008, WSDOT unpublished data). This information was used to identify high levels of mule deer-vehicle collisions (>10/year) along 5 distinct highway stretches, including State Route (SR) 20 in Okanogan County, situated within the Washington Department of Fish and Wildlife (WDFW) East Slope Cascades Mule Deer Management Zone (MDMZ)(WDFW 2016).

State Route 20 lies within the Methow Valley in Okanogan County, where Washington's largest wintering concentrations of migratory mule deer exist (Zeigler 1973). The majority (80 - 90%) of mule deer comprising herds in the Methow Valley are believed to migrate seasonally between alpine meadow and subalpine basin summer ranges along the Cascade Crest and lower elevation (<4,500 ft) winter ranges, such as the Methow Valley (Zeigler 1973, Myers et al. 1989). The Methow Valley supports mule and white-tailed deer, both of which have been implicated in deer-vehicle collisions in the area (WSDOT, unpublished data). Resident year-round mule deer herds also appear to be present (W. Myers, pers. comm.), as indicated by year-round deer-vehicle collisions (WSDOT, unpublished data). For these reasons, this region has received much attention with regard to deer-vehicle collisions. The WSDOT, in partnership with NGOs and other agencies, is working to identify where to install engineering solutions to reduce deer-vehicle collisions in this wildlife management zone, with a particular focus along SR 20 (WDFW 2016).
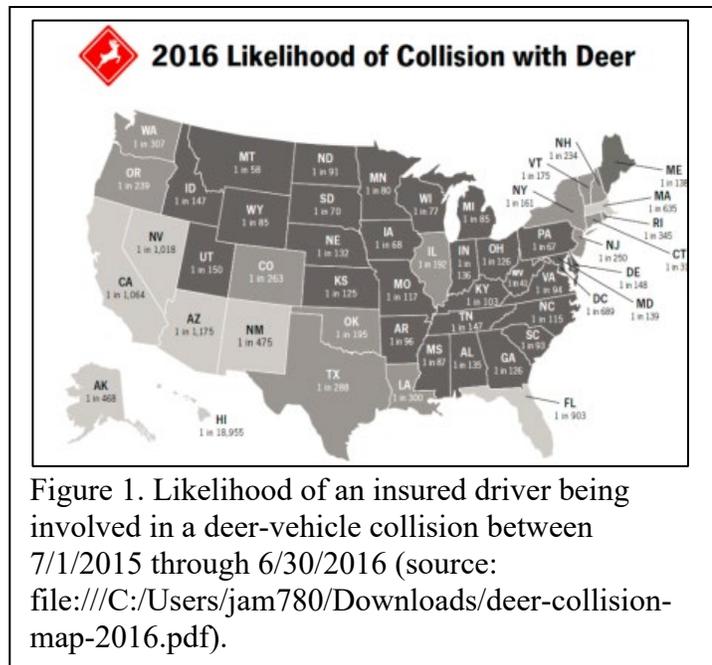
Figure 1. Likelihood of an insured driver being involved in a deer-vehicle collision between 7/1/2015 through 6/30/2016 (source: file:///C:/Users/jam780/Downloads/deer-collision-map-2016.pdf).

Deer-vehicle collision and carcass records collected across space and time provide a rich dataset from which to evaluate patterns and investigate habitat associations. Myers et al. (2008) analyzed deer-vehicle collision patterns in Washington State, described traffic levels, speed limit, and

roadside features influencing deer-vehicle collisions, and recommended that future studies focus on reviewing existing site-specific deer location data and mapping of sites where high levels of deer collisions are known to occur. These data document the occurrence of unsuccessful highway crossings, and additional information on successful highway crossings (i.e., when a deer crosses a highway without getting hit by a vehicle) can further improve our understanding of deer-vehicle collision risk and the success of engineering solutions intended to reduce deer-vehicle collisions and simultaneously minimize impacts to deer populations. For example, additional mapping of spatially explicit deer locations and counts along highways are necessary for differentiating between where deer successfully and unsuccessfully cross a highway. Such data, coupled with a detailed geodatabase of deer-collision data maintained by WSDOT, can be used to examine individual and interactive influences of vehicle traffic level and speed, as well as road geometry from the frequency of deer crossings. Using both sources of data can help inform engineering solutions and deer management strategies identified under the Washington Mule Deer Management Plan and Mule Deer Initiative (WDFW 2016).

To investigate competing hypotheses regarding various environmental and road geometry factors that may influence deer-vehicle collisions along SR 20 within the Methow Valley region, we: a) summarized existing deer carcass removal and deer-vehicle collision datasets, b) conducted a pilot study involving direct field observations, and c) completed a larger, main study that involved deploying remote game cameras, radio-collaring and tracking, and proximity sensor datalogger technology along the SR 20 right-of-way.

OBJECTIVES

General objectives were to:

1. Determine environmental factors associated with the frequency of deer-vehicle collisions
2. Expand our understanding of why deer-vehicle collisions occur
3. Provide management recommendations to reduce the frequency of deer-vehicle collisions

Specific objectives were to:

1. Quantify expected (mean) frequencies of deer-vehicle collisions along SR 20
2. Determine individual deer movements and use of SR 20
3. Assess status of historical and current mule deer migration corridors
4. Quantify roadway and roadside landscape and habitat features
5. Determine importance of landscape and local habitat features on the frequency of deer-vehicle collisions
6. Recommend locations for consideration of engineering solutions to minimize deer-vehicle collisions

STUDY AREA

The study area was comprised of the landscape surrounding Washington State Route 20 from Twisp, WA west to the U.S. Forest Service Early Winters Campground near Mazama, WA (Figure 2); this is slightly constrained from the original study area from Twisp to Rainy Pass.
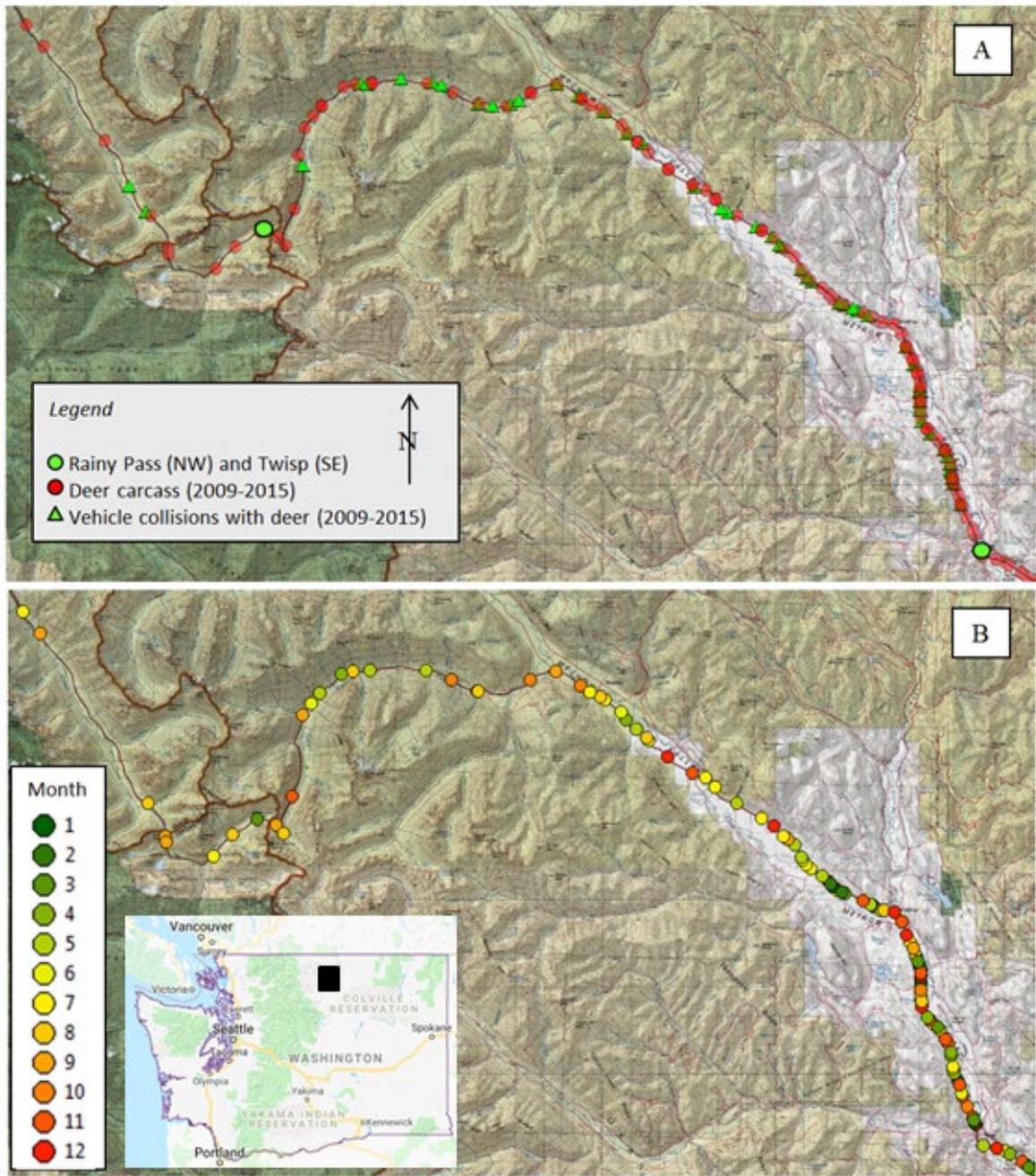
Figure 2. Study area, deer carcass and collision locations (a), and deer carcass locations by month (b) recorded by WSDOT from 2009-2015 along State Route 20 through the Methow Valley between Twisp and Rainy Pass, Washington.

Permits and Authorizations

All animal, capture, handling, and release activities associated with this study were approved and carried out under Washington State University Institutional Animal Use and Care Committee Animal Subjects Approval Form 04968, Washington Department of Fish and Wildlife (WDFW) Scientific Collecting Permit 17-339, and WDFW Right-of-Entry permit 110381,110366,110309, dated January 22, 2018. Field activities occurred on both, private and public lands with prior approvals. Private landowners were contacted, received a description of project activities, and granted authorization where activities took place on private lands. We posted signs at capture locations that described project activities, provided contact information, and coordinated activities with local US Forest Service and WDFW personnel.

SPATIAL AND TEMPORAL PATTERNS OF DEER-VEHICLE COLLISIONS

Existing Deer Carcass and Collision Databases

To summarize existing information on deer-vehicle collisions and inform the timing of sampling during the field component of this study, we used two existing geodatabases to quantify and examine spatial and temporal patterns of expected (mean) frequencies of deer-vehicle collisions: a) deer carcass data recorded by WSDOT personnel during carcass removal efforts from 2009-2015 ($n = 242$) and b) deer-vehicle collision incidents that were reported to state law enforcement from 2009-2014 ($n = 34$). From these data, frequencies of deer carcasses (mule deer and white-tailed deer combined) were calculated yearly and monthly in each 1-mile highway segment along the entire study area, and these were used to stratify highway segments into deer-vehicle collision frequency categories (low, medium, and high frequency) to develop stratified random sampling designs the main study presented below. Average monthly number of carcasses that were removed from 1-mile segments by WSDOT personnel were grouped and presented according to the biological seasons characterizing deer use of the study area: summer (Jun, Jul, Aug, Sept), fall migration (Oct, Nov), winter (Dec, Jan, Feb, Mar), spring migration (Apr, May).

Deer-vehicle collision incidents are typically an ideal data type for examining spatial and temporal patterns, but the low number of incident reports precluded a detailed assessment. This low number of deer-vehicle collision records was likely due to an underrepresentation of reports by drivers involved in a deer-vehicle collision where no vehicle damage or human injury occurred regardless of whether a deer was fatally injured. This bias may have contributed much to the weak relationship between these two datasets (Figure 3). Despite the low number of deer-vehicle collision reports, diurnal patterns of deer-vehicle collisions showed a distinct unimodal pattern through time of day, with a peak number of collisions occurring approximately 7 hours before and after noon (Figure 4).

The WSDOT carcass removal data were used to assess spatial patterns in deer-vehicle collisions by examining frequencies that occurred in each 1-mile segment (Figures 2 and 8). The number of carcasses removed increased southward from mile post 176, peaking near the town of Winthrop at mile 194 (Figures 5, 6, 7, and 8). Numbers declined southward from Winthrop to Twisp (mile 201) (Figure 5). This pattern did not hold across seasons, with peaks emerging around Winthrop and between Winthrop and Early Winters Campground during fall and spring migration periods

(Figure 6). Interestingly, the abundance of mule deer carcasses peaked between July and November, whereas the abundance of white-tailed carcasses peaked in December and January (Figure 7), revealing the different seasonal patterns of use by these two species in this area of the Methow Valley.
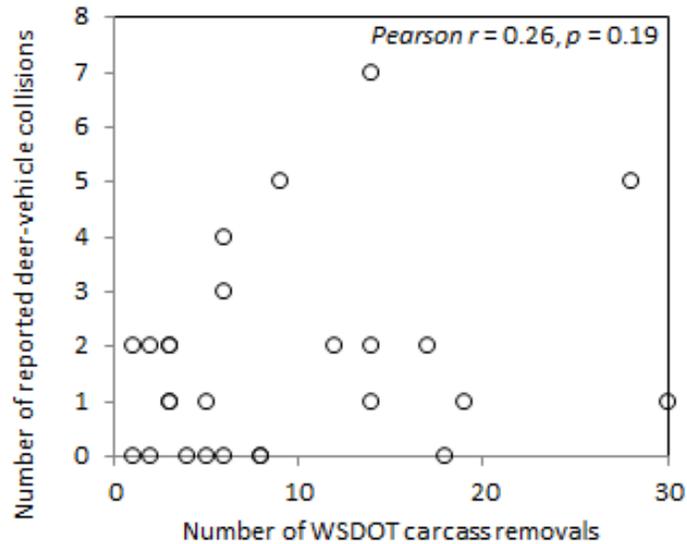
Figure 3. Scatterplot of reported numbers of WSDOT carcass removals ($n=241$) and deer-vehicle collision incident reports ($n=34$) between SR 20 mile markers 176-201 from 2009-2015. A correlation coefficient (r) is included.
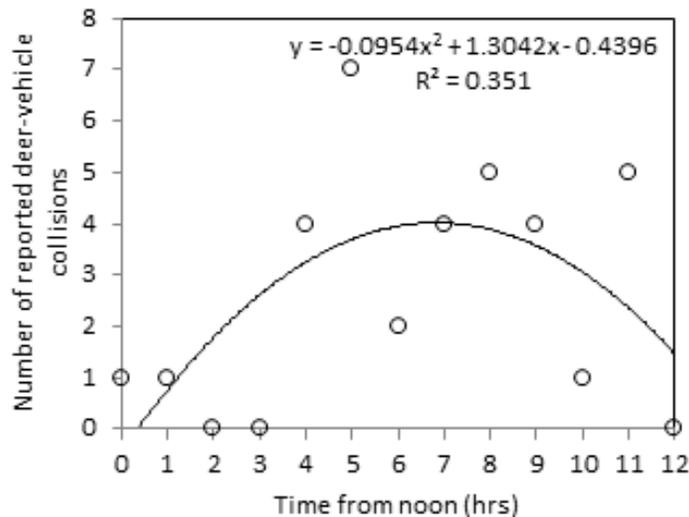
Figure 4. Number of reported deer-vehicle collision incidents ($n=34$) as a function of time + time^2 from noon (hrs) ($x = 0$ represents 12 noon, $x = 1$ represents both 1pm and 11am, $x = 6$ represents both 6pm and 6am, etc.). Data are from 2009-2014.
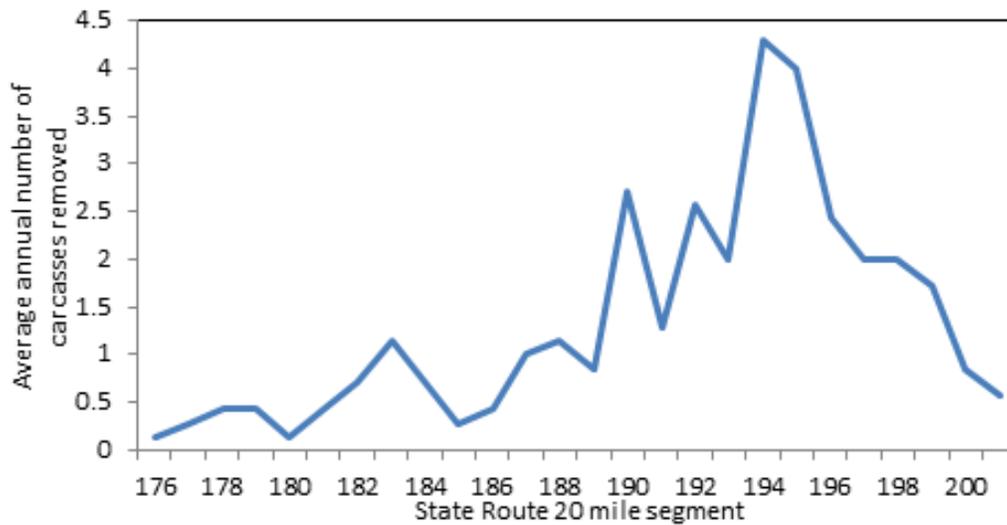
Figure 5. Average annual number of deer carcasses (mule deer (n=191) and white-tailed deer combined (n=51)) removed from 1-mile segments of SR 20 between mile markers 176-201 from 2009-2015.
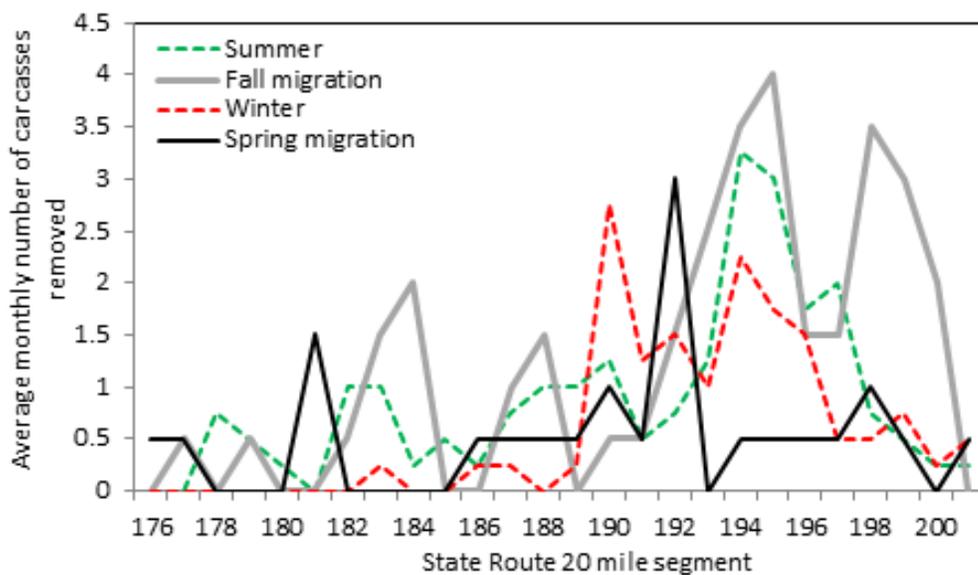
Figure 6. Average monthly number of deer carcasses (mule deer (n=191) and white-tailed deer combined (n=51)) removed from 1-mile segments of State Route 20 in the Methow Valley, Washington by WSDOT personnel from 2009-2015 according to season: summer (Jun, Jul, Aug, Sept), fall migration (Oct, Nov), winter (Dec, Jan, Feb, Mar), spring migration (Apr, May).
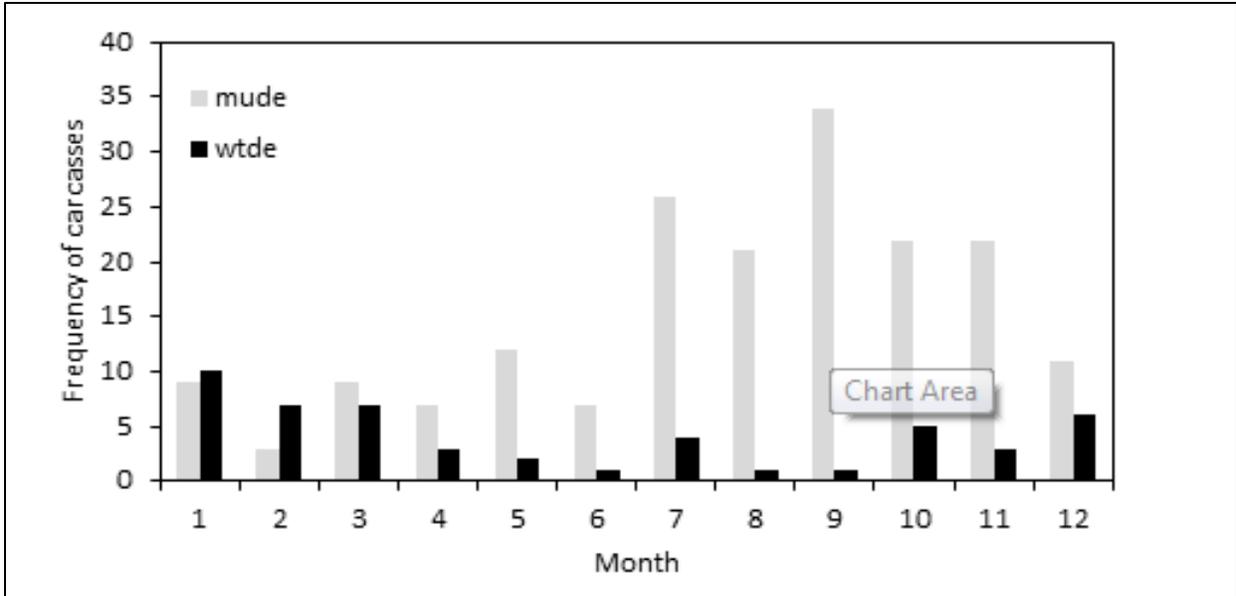
Figure 7. Frequency of deer carcasses (mule deer (n=191) and white-tailed deer combined (n=51)) removed from State Route 20 between mile posts 176-201 in the Methow Valley, Washington by WSDOT personnel from 2009-2015

Figure 8. Cumulative counts of deer carcasses removed from SR 20 in the Methow Valley by WSDOT between 2009-2015. Mile posts are shown. See Figure 5 for graphical representation of average annual counts.

Page 7

Previously Identified Mule Deer Migration Corridors

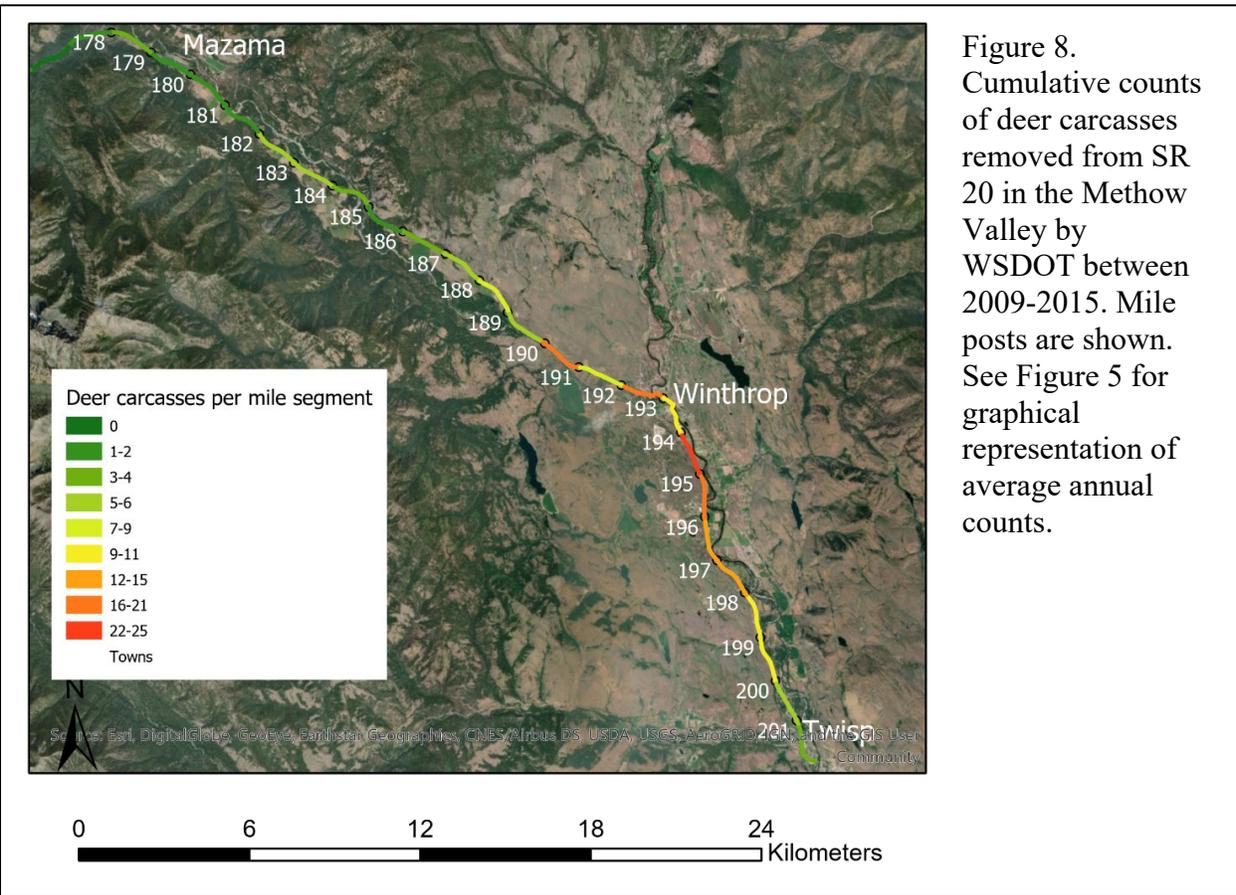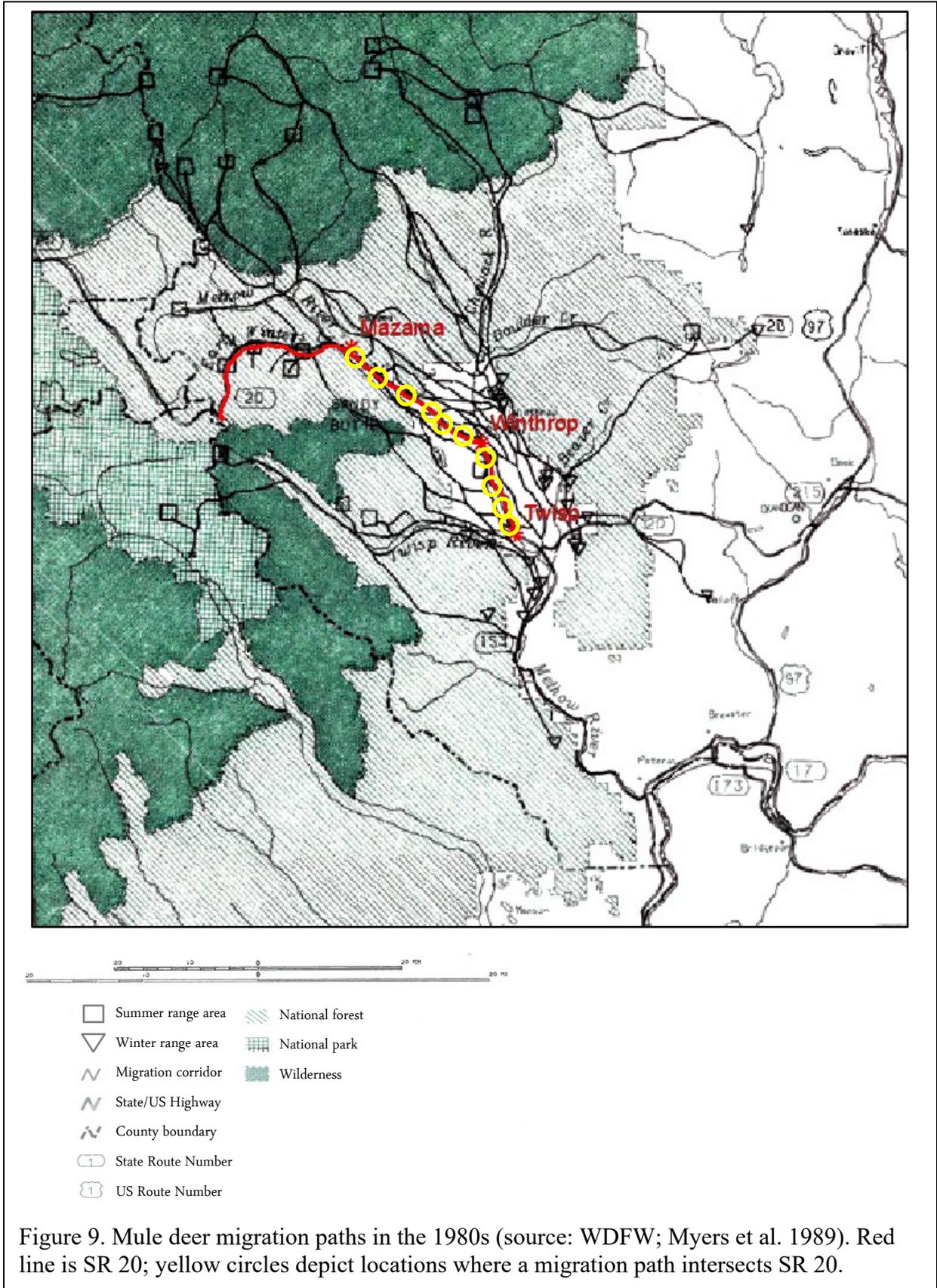The WDFW studied the seasonal movements of radio-collared mule deer in the Methow Valley and surrounding region in the 1980s, and mapped out summer ranges, winter ranges, and migration corridors (Figure 9; Myers et al. 1989). Summer ranges typically were distributed in higher elevation areas, although there was one summer range just southwest of Winthrop, immediately west of SR 20 between mile posts 195 and 197 (Figure 9). Winter ranges typically occurred in the valley bottom and surrounding low foothill areas from approximately 12 km north of Winthrop in the Methow Valley and Big Valley confluence to approximately 12 km south of Twisp. Based only on the sample of radio-collared deer available, the WDFW identified migration paths between summer and winter ranges that effectively traversed much of this landscape, indicating that this valley is a major and significant migratory corridor for the region's mule deer population. From the numerous migration paths identified by WDFW, 10 crossed SR 20 between Mazama and Twisp. However, given the high number and widespread distribution of migration paths in the valley, it is reasonable to expect that entire population of mule deer that overwinter in the valley and surrounding region move throughout much of the valley bottom and surrounding foothills to meet resource requirements (e.g., forage, water, thermal protection, avoid predation risk) during winter. This may also be the case in summer due to the presence of summer range in the valley.

Pilot Study

We conducted a pilot study during summer 2017 to investigate the extent to which deer-vehicle collisions were related to the frequency of live deer occurring along the SR 20 right-of-way. For this, we conducted simultaneous, foot-based visual surveys for live and dead deer weekly from May through August 2017. This time of year was chosen because preliminary findings from the existing databases referenced above revealed a peak in mule deer carcass removals between July and November. A single observer recorded standardized data for 1 hour / week in each 1-mile section, and reported the species, status (live or dead), number, status of road crossing (crossing or not crossing SR 20), and coordinates of each encounter. These data were then combined into their corresponding 1-mile SR 20 segments, and used to compare the frequency and cumulative counts between the two species, the probability of deer crossing the road and the average number of live deer, and number of carcasses and number of road crossings in each 1-mile section.

Between May and August 2017, a total of 835 animal observations were recorded (Figure 10a), with 29 of these documented as carcasses attributed to wildlife-vehicle collisions (Figure 10b). Of these, 537 mule deer and 229 white-tailed deer were observed. Numbers of live deer varied spatially, with peak counts centered around the town of Winthrop (Figure 11).

The frequency and cumulative counts of mule deer and white-tailed deer were negatively correlated (Figure 12). The probability of deer crossing was correlated to the average number of live deer (Figure 13a), and the number of crossings was predicted by number of live deer (Figure 13b). However, number of deer carcasses was unrelated to the frequency of road crossings after accounting for WSDOT carcass removal and WDFW citizen salvage (Figure 14).

Figure 9. Mule deer migration paths in the 1980s (source: WDFW; Myers et al. 1989). Red line is SR 20; yellow circles depict locations where a migration path intersects SR 20.
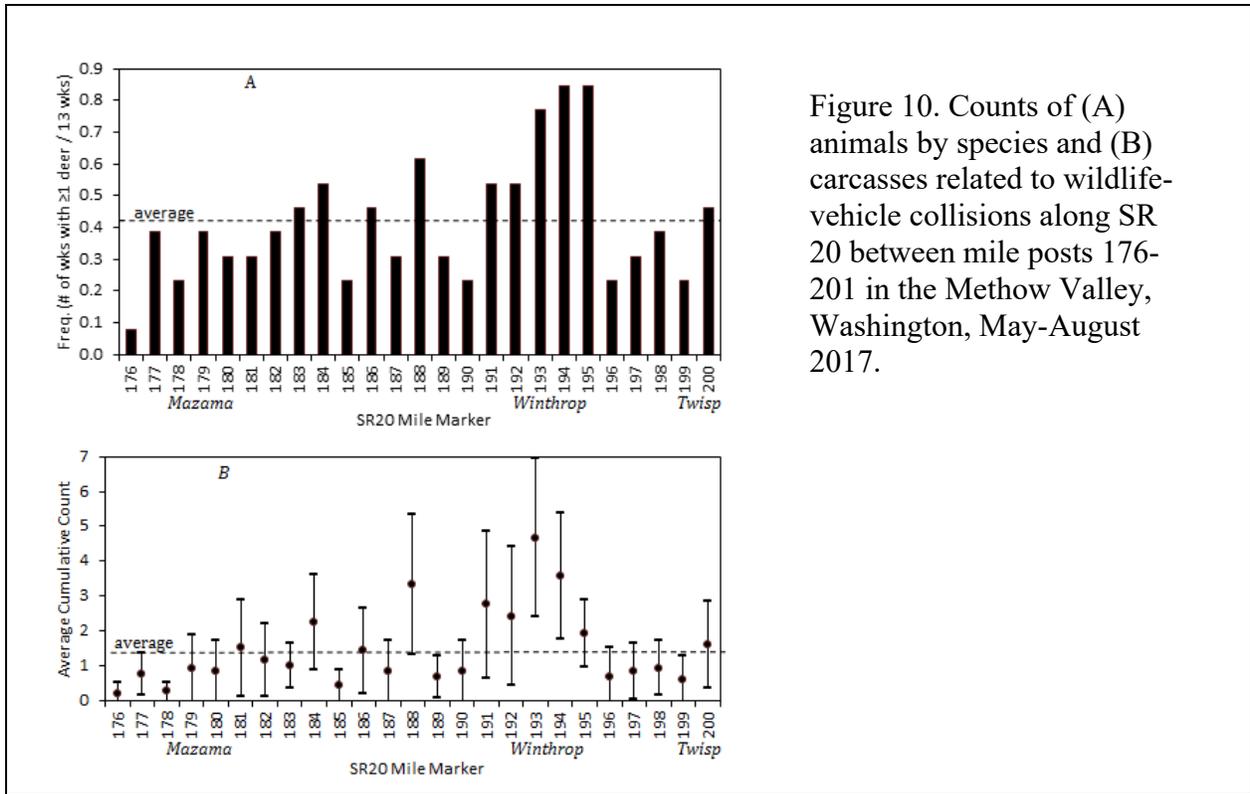
Figure 10. Counts of (A) animals by species and (B) carcasses related to wildlife-vehicle collisions along SR 20 between mile posts 176-201 in the Methow Valley, Washington, May-August 2017.
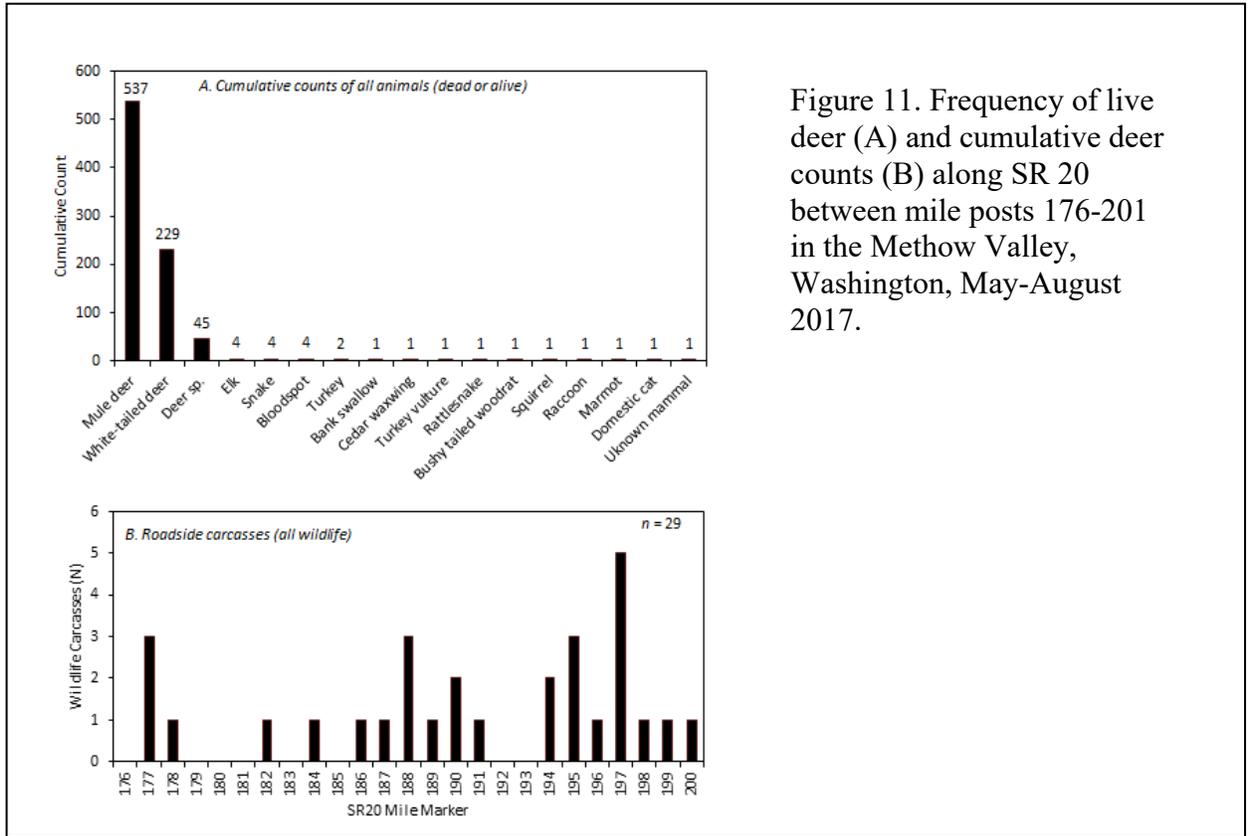
Figure 11. Frequency of live deer (A) and cumulative deer counts (B) along SR 20 between mile posts 176-201 in the Methow Valley, Washington, May-August 2017.
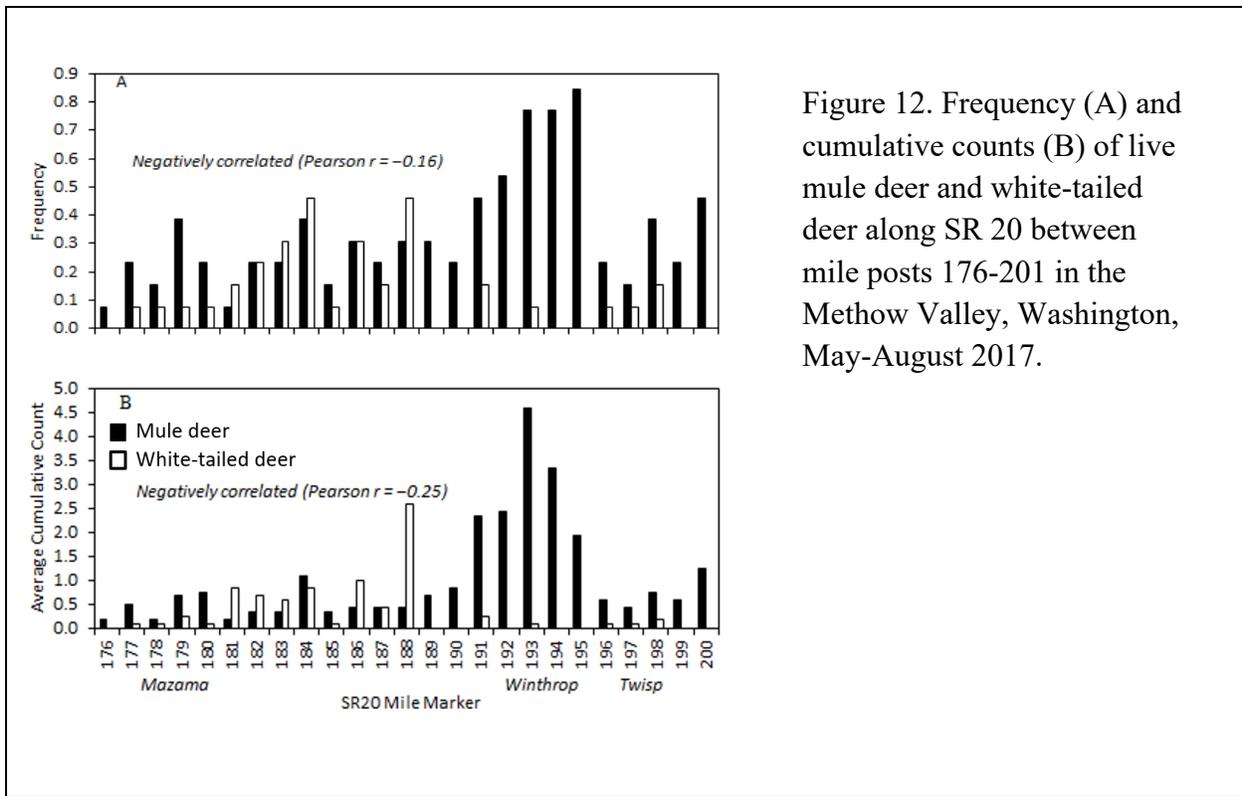
Figure 12. Frequency (A) and cumulative counts (B) of live mule deer and white-tailed deer along SR 20 between mile posts 176-201 in the Methow Valley, Washington, May-August 2017.
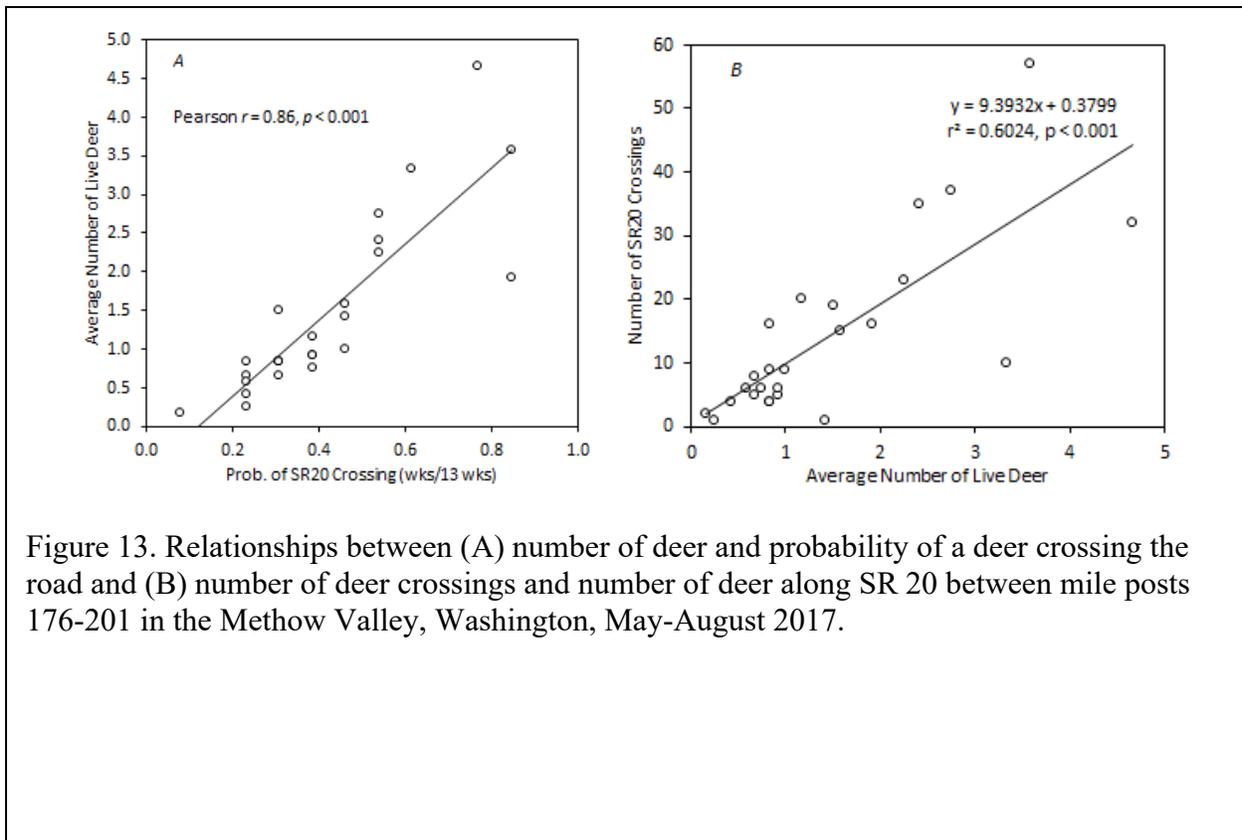
Figure 13. Relationships between (A) number of deer and probability of a deer crossing the road and (B) number of deer crossings and number of deer along SR 20 between mile posts 176-201 in the Methow Valley, Washington, May-August 2017.

Figure 14. Relationship between live deer crossings and deer carcasses after accounting for carcasses that were removed by WSDOT and WDFW citizen salvage permits along SR 20 between mile posts 176-201 in the Methow Valley, Washington, May-August 2017.

MODELING ENVIRONMENTAL DRIVERS OF DEER-VEHICLE COLLISIONS

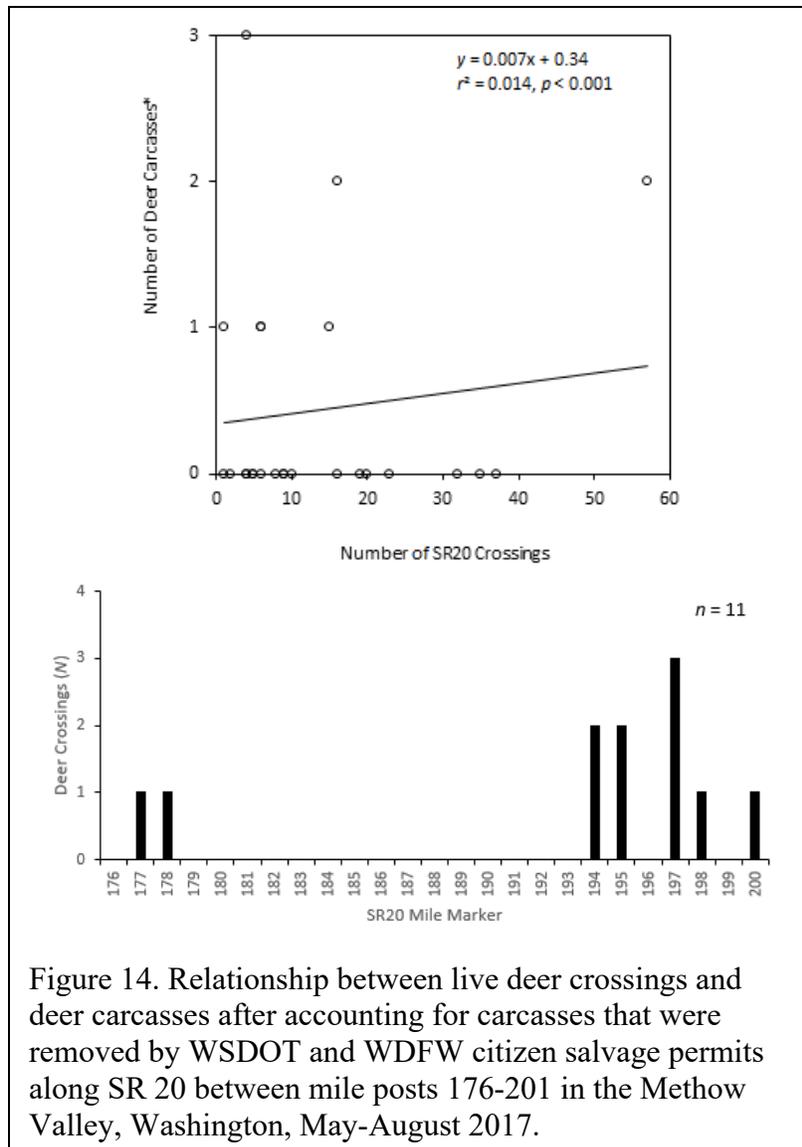## Field Sampling and Predictor Datasets

Frequency of deer-vehicle collisions (standardized carcass surveys)

<u>***Spring and fall carcass surveys***</u> -- Information on the distribution of carcasses along the highway was gathered to calculate empirical estimates of carcass abundance. This sampling design included repeat surveys that allowed for correcting unintentional bias that can emerge from imperfect detection of carcasses during surveys or incidental carcass removal efforts (e.g., detection <100% because some carcasses may go undetected by some observers due to being obstructed by vegetation, topography, degree of decomposition, distance from asphalt, etc.).

Carcass surveys were conducted following standardized survey methods in mid-spring (April 15 and 22) and mid-fall (October 21 and 28), 2017 by WSU Pullman Campus' SOE 446 Wildlife Habitat Ecology students. Surveys entailed walking both sides of the highway in pairs across the entire study area between 0900 and 1400 h to detect and record the condition and location of each detected deer carcass. Fresh carcasses and skeletal remains confirmed to be deer (i.e. the presence of skin, teeth, antler, or a skull) were recorded as carcasses and identified to species when possible (white-tailed deer, mule deer, or deer sp.). The mid-spring survey included recording deer tracks and scat, and the fall survey included assigning the state of decomposition into 1 of 3 categories: 1) old carcass, which were carcasses that consisted only of bones or bones and dried skin and fur (these were assumed present during the April survey), 2) possibly recent carcass, with aged and dried flesh and skin (possibly deposited since the April survey), and 3) recent carcass, which were freshly killed deer with un-desiccated flesh (deposited since the April survey). Thus, the spring survey represented the baseline of all carcasses present in the study area at that time, including those from past years that remained in a skeletal state and bone piles. The raw count was 177 in April and 233 in October (Figure 15).

We used these April and October 2017 carcass data to determine how many and where new carcasses emerged (as a proxy for deer-vehicle collisions that resulted in deer mortality) in the study area during this period. For this, we first identified and removed repeat detections of April carcasses (i.e., those October carcasses <5 m from an April carcass). We considered October carcasses that were classified as recent as a new carcass regardless of being <5 m from an April carcass, and retained these recent records in the data. If >1 October carcass was <5 m from an April carcass, we only removed the closest October location, producing a raw count of 192 new carcasses.

To ensure that the 2017 summer data captured the general spatial patterns in carcass abundances and were suitable for subsequent modeling, we compared our raw counts of new carcasses from summer 2017 to the cumulative WSDOT counts between 2009-2015. A general pattern of higher raw counts corresponding with higher carcass counts recorded by WSDOT between 2009-2015 did emerge, albeit with the 2017 summer survey detecting an average of 25% less carcasses as expected (Figure 16). This lower number of carcasses compared to that recorded by WSDOT was expected because WSDOT removes recorded carcasses from the highway. It is reasonable to expect an even lower percentage to have been detected in a single summer survey compared to

the 6 years of WSDOT data, but we attribute the absence of this to the 2017 summer survey extending outward from the center line across to include the entire width of the right-of-way width where many deer likely moved to before dying after a deer-vehicle collision and not recorded by WSDOT.

Correcting for carcass detection bias -- To construct models and test hypotheses regarding factors that influence deer-vehicle collisions, reliable estimates of carcasses were needed for use as a proxy for the number of deer-vehicle collisions that resulted in deer mortality. Since estimated abundances of carcasses along SR 20 can be influenced by the observer's ability to detect (see) carcasses, we estimated and corrected for imperfect detection of carcasses during visual surveys. During the 2017 spring carcass survey, a set of consecutive 1-mile segments was randomly selected for mark-resight sampling (McClintock et al. 2009) during two separate carcass survey occasions on the same day, such that two groups of observers surveyed the same randomly selected sample of three 1-mile-segments of SR 20 independent of each other. From these data, a carcass detection rate (d) was calculated for the spring survey effort as $d = k/(c \times t)$, where k is the number of times the number of carcasses (c) were detected over $t = 2$ surveys; here, the detection rate can range from 0 (no detection of carcasses) to 1 (100% of carcasses detected on both mark-resight surveys).

The probability of detecting a carcass was estimated to be 0.69, and the probability of not detecting a carcass that was present was estimated to be 0.31 (1-0.69). Applying these probability statements, we corrected for false positive detections (carcasses present but missed in April and detected in October; (1-0.69)*0.69 = 0.21) and overall detection rate (0.69) in the raw count of new carcasses ($n = 192$), producing a mark-resight detection bias corrected estimate of 219 new carcasses along the SR 20 right-of-way attributed to deer-vehicle collisions that resulted in deer mortality. From this, we produced spatially explicit estimates of detection bias corrected estimates of new carcass abundance, which also showed a comparable pattern in carcass abundances documented across the study area between 2009-2015 by WSDOT (Figures 16 and 17), indicating that the 2017 summer data were suitable for modeling the deer-vehicle collision process in this area of SR 20.

Figure 15. Results from deer carcass surveys between mile posts 176-201 in the Methow Valley, Washington in A) mid-spring (April) 2017 and B) fall (October) 2017.
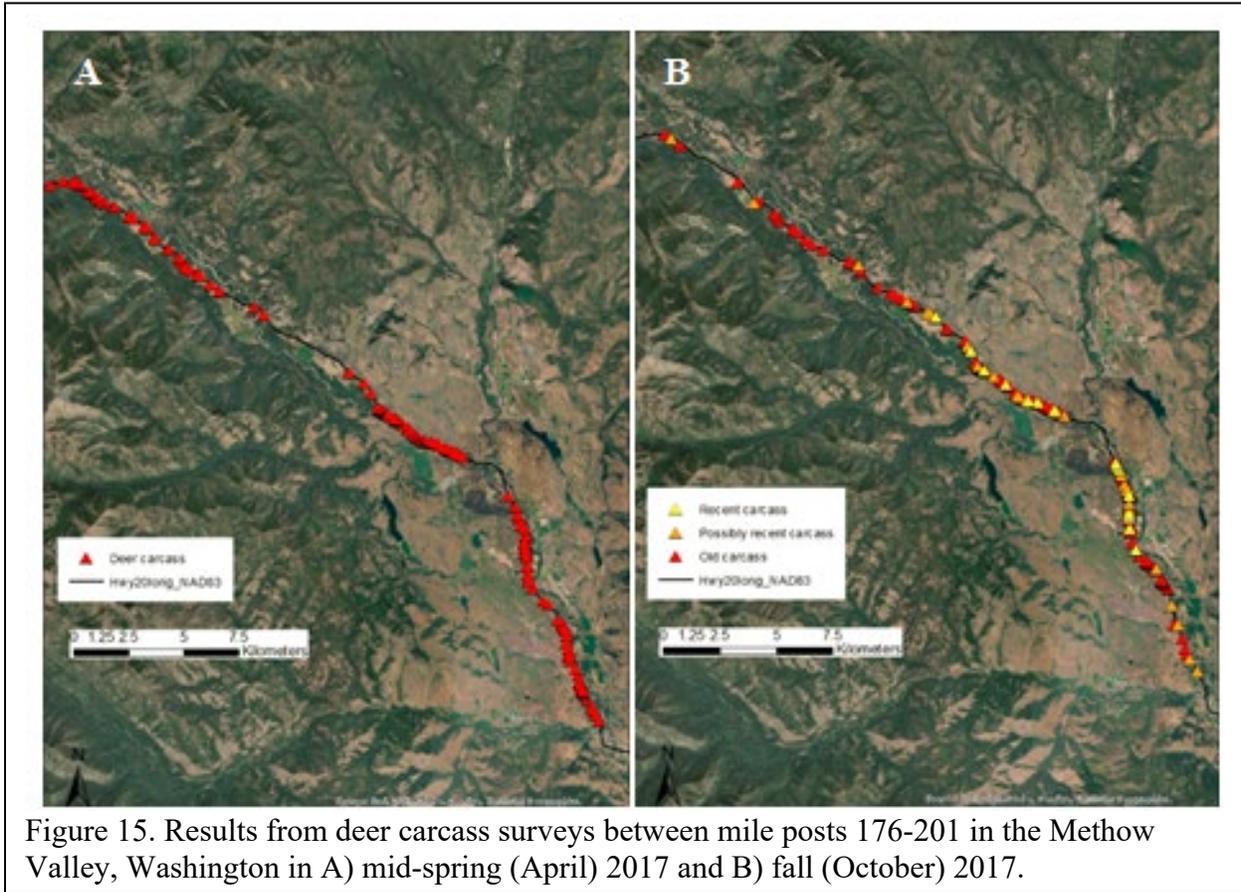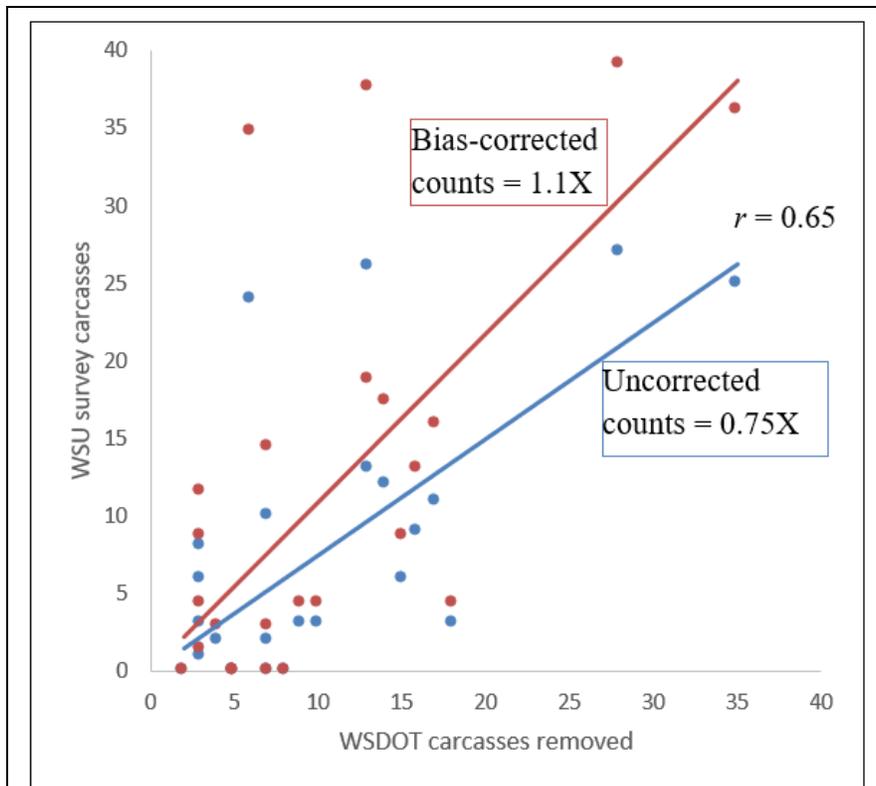
Figure 16. Counts of new deer carcasses detected between April and October 2017 compared with counts of carcasses removed by WSDOT 2009 – 2015 between mile posts 176-201 of SR 20, Washington. Carcasses counted in 1-mile segments (sampling units here) centered around mile posts. Uncorrected counts are raw counts; bias-corrected are raw counts corrected for detection bias (0.69).
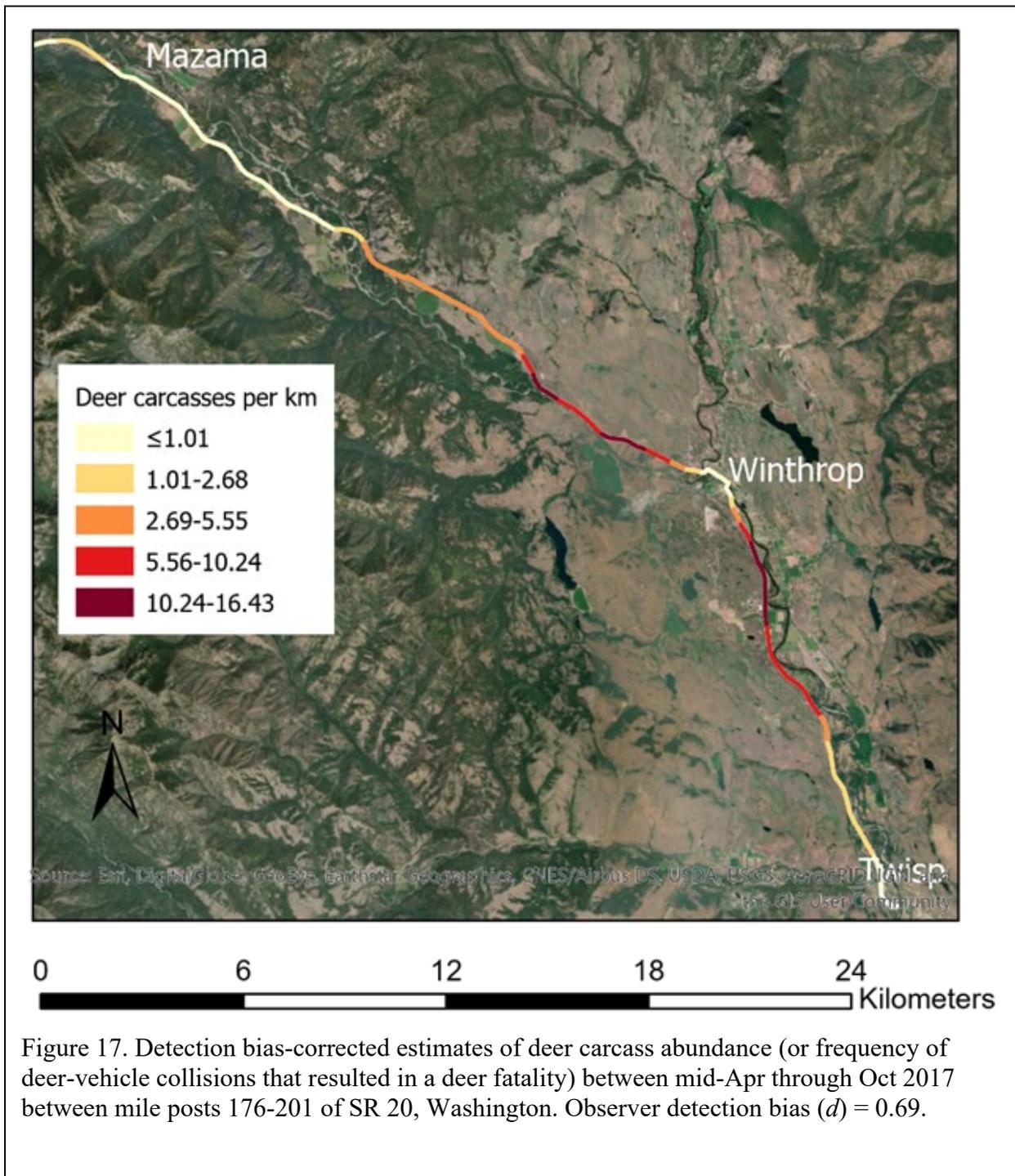
Figure 17. Detection bias-corrected estimates of deer carcass abundance (or frequency of deer-vehicle collisions that resulted in a deer fatality) between mid-Apr through Oct 2017 between mile posts 176-201 of SR 20, Washington. Observer detection bias (d) = 0.69.

Frequency of SR 20 crossings by deer (game cameras)

Browning Dark Ops Elite BTC-6HDE game cameras (n = 60) were deployed along SR 20 (3/mile) in a stratified random sample of 1-mile road segments according to the frequency of deer carcasses to examine the presence/absence of deer along the right-of-way within study area.

Cameras were installed in April 2017 and removed in October 21, spanning the peak months when previous deer-vehicle collisions have occurred. Cameras were set to record a single photograph when triggered by an animal's movement or heat signature. Photo processing included the assignment of each photo to species and count of individuals. Photo processing was completed by students enrolled in the WSU Pullman Campus' SOE 446 Wildlife Habitat Ecology course in Fall 2017 and 2018.

Of the 60 cameras deployed, one malfunctioned and did not record data. A total of 519,284 georeferenced, time-stamped photographs were recorded by the 59 game cameras from April – October 2017. Photos were processed/sorted into 18 species groupings (Appendix A; Figure 18). The species with the highest frequency of photographs was mule deer ($n = 4,855$), followed by unknown deer species (i.e., deer species not distinguishable) ($n = 1,467$), and white-tailed deer ($n = 1,118$).

Figure 18. Number of photos of A) mule deer and B) white-tailed deer recorded by game cameras per day along SR 20 in the Methow Valley, Washington from April - October 2017. Mile posts are shown.
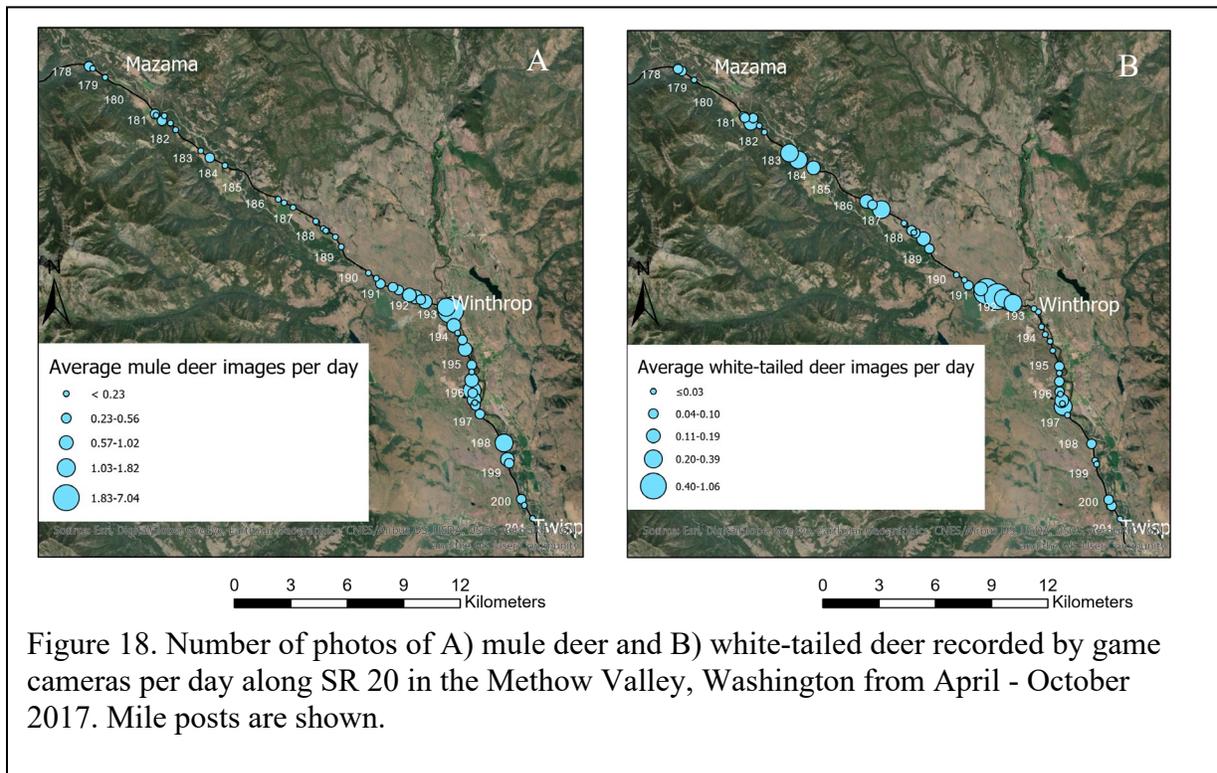
Movements and frequency of SR 20 crossings by individual deer (radio-tracking and data loggers)

Deer capture and radio-collaring -- To convert frequency of deer crossings (from game cameras described in the section above) to estimates of deer abundance, we captured and radio-collared deer to quantify movements and the number of SR 20 crossings by individual deer. Deer were captured in baited Clover traps (Clover 1954, 1956, Thompson et al. 1989, VerCauteren et al. 1999) from January 1 through March 31, 2018 in close proximity to the SR 20 right-of-way

(Figures 19 and 20). We constrained our capture effort to this winter period to minimize risk of deer experiencing hyperthermia and negative effects on pregnant females during spring (Casady and Allen 2013), and because the WDFW required this time period for these reasons. Capture areas were selected based on a combination of topography, vegetation, winter range designation and presence of deer during our trapping effort, access, and distance to SR 20. To increase independence of samples, we initially distributed our capture efforts throughout the study area and applied trapping effort in proportion to observed abundances prior to this period, where areas with higher numbers of deer were targeted for greater numbers trap nights. We also distributed traps in several areas where white-tailed deer were more abundant to account for the proportion of white-tailed deer vs. mule deer involved in collision from 2009-2015 (18% white-tailed deer). An observed absence of deer in the northern half of the study area as early as mid-January (due to increased snow accumulations in the Mazama area) led to adjusting our capture efforts to the southern half of our study area (Figure 20), which supported primarily mule deer.

Clover traps were baited with apples soaked in a brine solution. Traps were checked 3 times per day, and males and fawns were immediately released without handling or collaring in order to minimize health risk associated with placing a collar on an animal that may experience a changing or growing neck circumference. Adult female deer were physically restrained, hobbled, and blindfolded without immobilization drugs, and released immediately after receiving a radio-collar and health assessment. Once an animal was released, we monitored the recovery process. All animal handling was conducted in accordance with guidelines and requirements from the WSU Institutional Animal Use and Care Committee Animal Subjects Approval Form 04968, Washington Department of Fish and Wildlife (WDFW) Scientific Collecting Permit 17-339, and WDFW Right-of-Entry permit 110381,110366,110309, dated January 22, 2018.

A total of 22 adult female deer (20 mule deer and 2 white-tailed deer) were fitted with a lightweight Vertex Plus radio-collar (Vectronic Aerospace GmbH). Collars were equipped with very-high frequency (VHF) transmitters, ultra-high frequency (UHF) transmitters, and morality sensors. All collars contained a decomposable cotton connector designed to allow collars to automatically drop off, except in cases where a deer died before that time. In cases where the mortality sensor was activated, the carcass was located, collar retrieved, and cause of death determined (where possible).

Radio-tracking -- All collared deer were radio-tracked using handheld R1000 VHF receivers (Communications Specialists, Inc.), directional RA-23 antennas (Telonics), and compasses (Silva) during regular intervals throughout the remainder of the trapping period (April 2018). From May through mid-August 2018, we continued to radio-track collared deer that remained in the valley during summer (i.e., non-migratory residents). We focused on summer tracking to target the period of peak mule deer-vehicle collisions (mid-summer) identified in the existing WSDOT deer carcass and collision data. Additionally, we used a combination of homing and triangulation for tracking (repeatedly relocating collared deer) during one day in October 2018 and 2019. Over the course of the study, >5,000 compass bearings to collars were recorded. Three bearings (each from a different location) recorded <1 hour apart (2,624 bearings) were used to generate triangulated locations of collared deer using Location Of A Signal (LOAS) software (Ecological Software Solutions LLC). A total of 2,624 bearings were included to estimate

triangulation locations, with bearings with low precision (e.g., in opposite direction from and not crossing the other two bearings attributed to 'bounce') excluded.

Migratory status of radio-collared deer -- Thirty-two percent (*n* = 7) of the 22 collared deer were not detected in the Methow Valley after May 2018 and presumed to have migrated to distant summer ranges. The remaining 68% (*n* = 15) were classified as "non-migratory;" these animals stayed in the study area after May 2018 (considered to be summer residents). This pattern, where approximately three quarters of sampled female deer exhibit a non-migratory life strategy, is not commonly reported in ungulate populations elsewhere in the north because elevational migration to lower-elevations are necessary for animals to survive deep snows associated with northern winters (Hebblewhite and Merrill 2009, Manning 2010, Anderson et al. 2012, Manning and Garton 2012, Middleton et al. 2013, WDFW 2016).

Radio-tracking of these remaining 15 resident deer took place from May through August 2018, with a total of 807 triangulation locations estimated (Figure 20). In October 2018 and 2019, triangulation was attempted in the study area for all 22 deer, with five (4 mule deer and 1 white-tailed deer) of those not detected in summer 2018 being detected. The other two collared deer that left the study area in May 2018 were not detected again, indicating that up to 32% (7) of the 22 collared animals were migratory.

Mortality status of radio-collared deer -- Five of the 22 collared deer died during the study; discovered by mortality signals and incidental sightings by local community members (Figure 21):

- White-tailed deer 6995 (radio frequency 264) died alongside SR 20 in May 2018, but extreme radio signal bounce prevented locating the carcass. This animal was captured and collared on March 27, 2018 in good body condition, albeit with a heavy lice load. Based on the strongest signals, it appeared that the animal died alongside SR 20 where the river abutted a turnout, indicating that it may have been involved in a deer-vehicle collision. However, it is unknown whether the heavy lice load or a collision with a vehicle was the ultimate cause of death.
- Mule deer 6996 (radio frequency 275) died next to Liberty Bell High School / Methow Valley Elementary School around January 10, 2019. Photos and general location provided by local resident. Cause of death unknown; much of carcass consumed by scavengers. But, its close proximity to SR 20 may indicate deer-vehicle collision.
- Mule deer 6962 (radio frequency 589) died south of Winthrop approximately 600 feet east of Twisp-Winthrop Eastside Rd on December 27, 2019. Residents detected the carcass after seeing avian scavengers, and WDFW biologist Scott Fitkin conducted a site visit and determined cause of death to likely be deer-vehicle collision due to proximity to road.
- Mule deer 6966 (radio frequency 815) died on SR 20 as a result of a deer-vehicle collision on August 13, 2019. University of Washington graduate student Lauren Satterfield observed and reported the mortality.
- Mule deer 6970 (radio frequency 014) died on SR 20 on or before November 4, 2019. Radio-collar dropped off at the WDFW office in Winthrop with site coordinates provided by local resident. Cause of death unknown, but location on SR 20 may indicate deer-vehicle collision. This deer was seen in the area on October 19, 2019 with two fawns.

Ultra-high frequency data logging system -- To convert the frequencies of deer crossings (from game cameras) to estimates of deer abundance, we established an automated UHF data logging system (*n* = 49 data loggers) within the SR 20 right-of-way to detect radio-collared deer and quantify the number of SR 20 crossings by individual deer. This system received the UHF frequency signals from radio collars and operated from January - October 2018. Each data logger automatically recorded information on radio-collared deer 24/7 when they entered <130m from a data logger (130m radius circle = 6 data loggers for complete coverage along highway in a 1-mile segment). Each data logger was set to record the ID, date, time, and location of individually radio-collared deer (see below) every 30 seconds while a deer was within the detectable range. In combination with the mortality of white-tailed deer ID 6995 in May 2018 and the migratory status of 7 deer, 14 collared animals were present in the study area from May – October 2018 and used for these analyses. Of the 49 data loggers deployed, 39 detected radio-collared deer during the study, ranging from 2 to 1,047 total detections per data logger (Figure 22).

Figure 19. Erecting a Clover trap and releasing a recaptured radio-collared adult female deer in the Methow Valley, winter 2018.
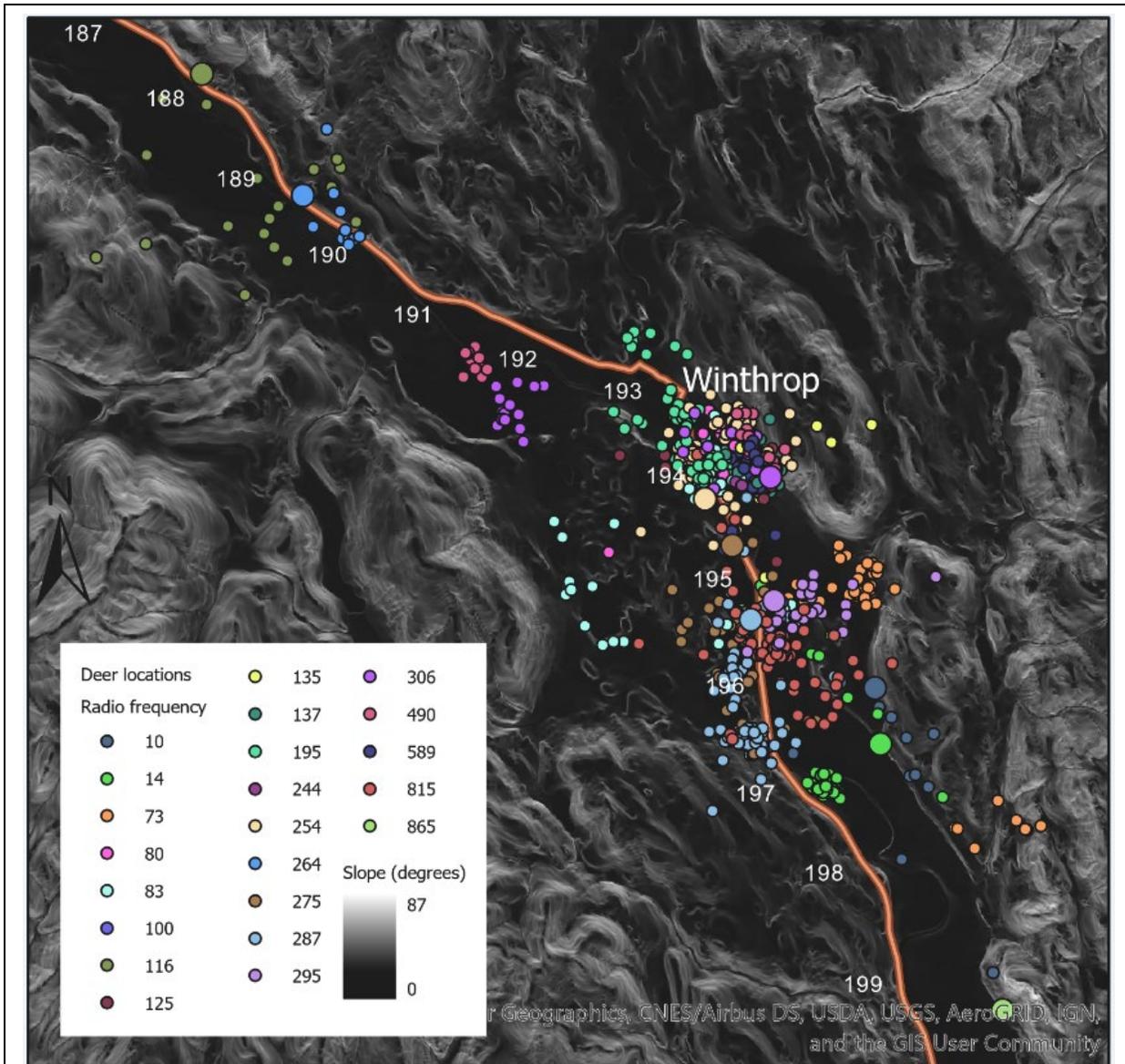
Figure 20. Radio-tracking Point locations (small circles) of radio-collared adult female deer estimated from VHF triangulation in the Methow Valley, January – August 2018. Larger circles are capture locations. Some capture locations represent multiple individuals. Additional trapping locations occurred, but without capture success.
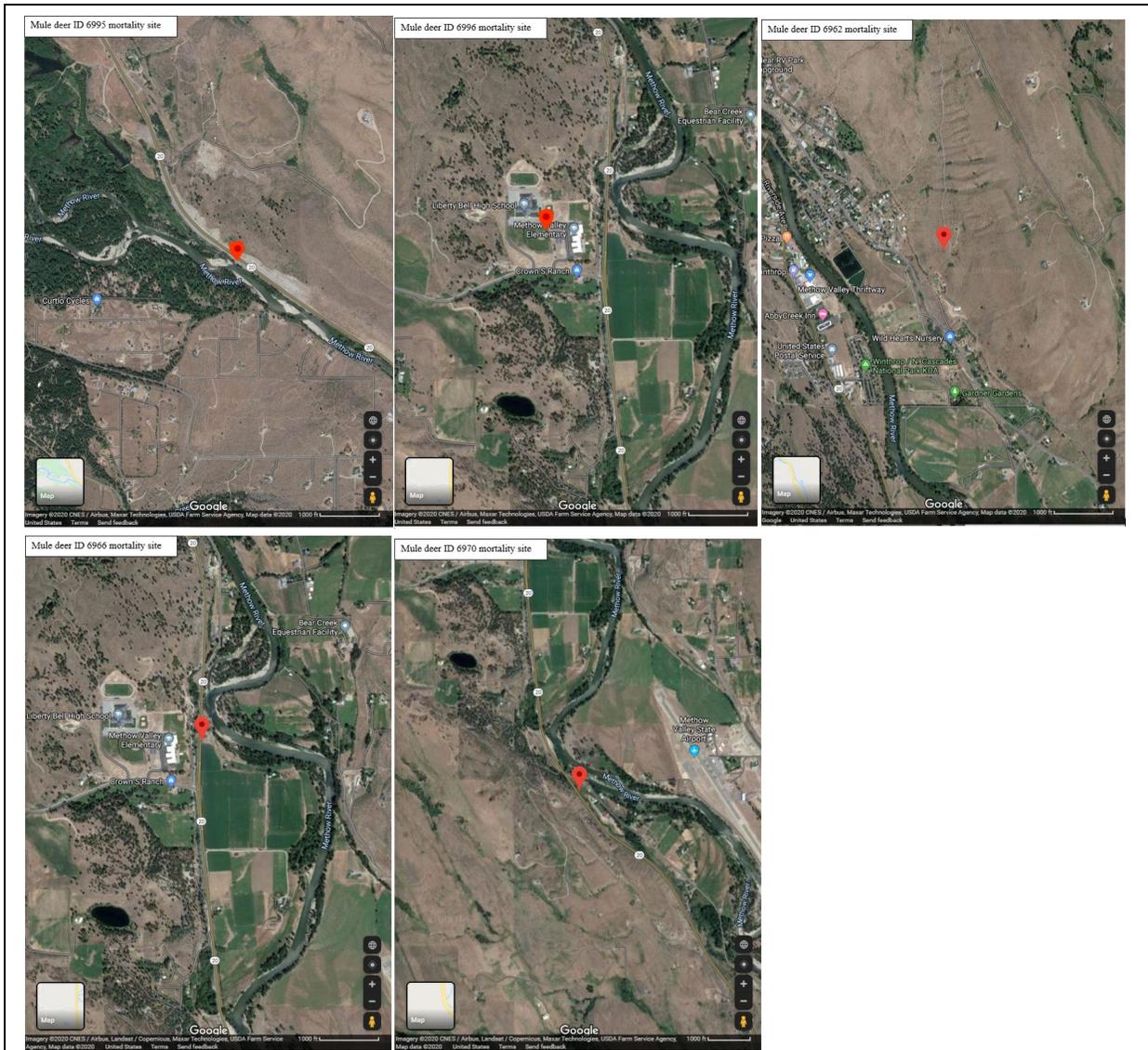
Figure 21. Mortality sites of radio-collared mule deer (n = 4) and white-tailed deer (*n* = 1), Methow Valley, Washington, 2018-2019. The 5 deer were white-tailed deer ID 6995 (radio frequency 264), mule deer ID 6996 (radio frequency 275), mule deer ID 6962 (radio frequency 589), mule deer ID 6966 (radio frequency 815), mule deer ID 6970 (radio frequency 014).
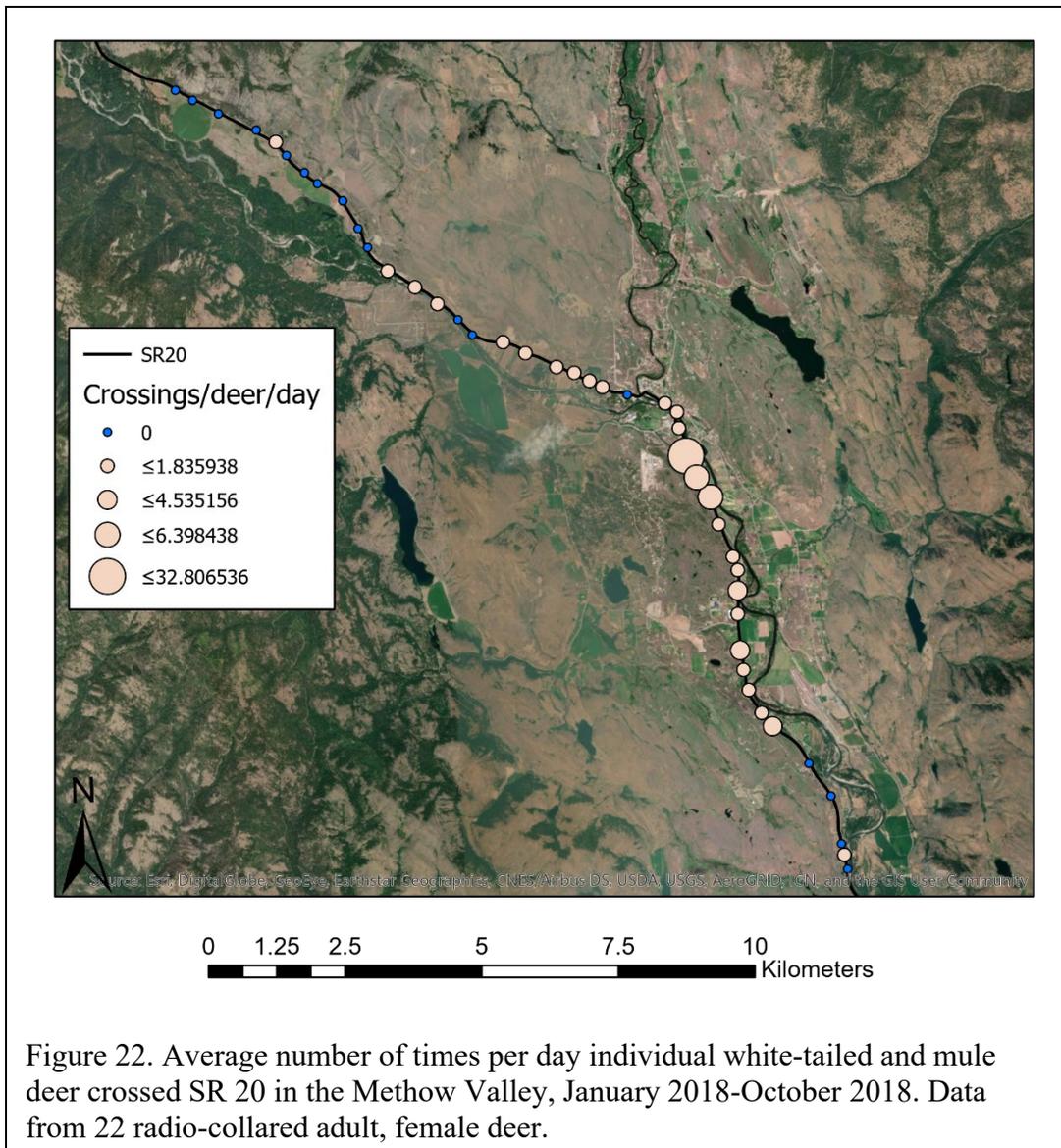
Figure 22. Average number of times per day individual white-tailed and mule deer crossed SR 20 in the Methow Valley, January 2018-October 2018. Data from 22 radio-collared adult, female deer.

Environmental variables

A series of landscape and habitat variables were considered as potential contributing factors of the deer-vehicle collision process and predictors in subsequent modeling. Two existing sources of land cover data were examined for accuracy in predicting vegetation that could be used to quantify environmental features in the study area. These two freely available datasets are the GAP Land Cover database and the National Land Cover Map (Homer et al. 2015, USGS 2011). This assessment was necessary because these maps were developed across broad regions at scales that may not yield the level of detail desired when linking local vegetation characteristics to individual wildlife movements and locations. To assess the accuracy of these two land cover maps, vegetation characteristics were recorded at 446 ground-truth locations across the study area and compared to that predicted by the maps. Of these, 320 locations were collected near the highway in April 2017 by students enrolled in the WSU Pullman Campus' SOE 446 Wildlife

Habitat Ecology course, and the remaining 126 were collected away from the highway during subsequent summer months by a WSU student intern.

Comparison of the vegetation recorded at ground-truth points with that predicted by the GAP and National Land Cover maps indicated that these two existing maps had a high level of error in classifying vegetation at local sites in the study area. Therefore, we used the more accurate map (National Land Cover) to create a baseline forest layer as a shapefile, then edited this layer within 5 km of the highway for accuracy, as well as hand-digitizing buildings, water features, and agricultural fields based on World Imagery (0.3m resolution) in ArcGIS Pro 2.4.1 (ESRI, Inc.) as of July 2019 (Figure 23). We considered three water categories: linear (canals and rivers), standing water (ponds and lakes), and all water features combined. We assumed that these all functioned as drinking sources for deer, but accessibility by deer differed. For example, canals and rivers both provided fresh water typically parallel SR 20, whereas standing water offered more remote sources of unknown quality (e.g., sewage or runoff) and accessibility (e.g., fencing, livestock competition, higher elevations, or farther from the highway). We considered all water features combined in order to account for the closest source of water regardless of type.

We created raster surfaces (10 m pixel size) of distance to different resources anticipated to influence deer space use (and possibly frequency of highway crossings in order to obtain required resources) using the Euclidean Distance tool in ArcGIS Pro 2.4.1. From the land cover map, these resources included forest patches >1500 m^2 to represent those that would provide thermal protection for deer during warm summer periods and severe winter conditions, buildings where lawns may attract deer to forage or humans and dogs may deter deer but also afford protection from large predators, agriculture as a source of food, and water resources as described above. We also measured distance from south-facing slopes without forest cover in patches >1000 m^2 (open south-facing slopes) as an important forage and thermoregulatory resource (direct solar radiation in winter reduces snow depth and aids in thermal requirements). We classified areas of the road that were juxtaposed between the nearest water, agriculture, and open south-facing slopes because hypothesized that this landscape position may increase the frequency of crossings, and hence deer-vehicle collisions.

We also created a raster surface of maximum slope at a fine-scale resolution along SR 20. For this, we characterized the slope along SR 20 at a 10-m resolution in degrees, based on a Digital Elevation Model (DEM; 1/3 arc-second, approximately 10 m pixels, USGS) and using the Slope tool in ArcGIS Pro 2.4.1. We then found the maximum slope within 60 m of each pixel using the Focal Statistics tool, which uses a moving neighborhood to characterize cells across the landscape. This surface was used to test the hypothesis that deer movements (e.g., a deer heading down a steep hill toward SR 20 may be less able to be seen and also less able to stop upon entering the road, whereas deer heading up steep slopes to the road may not be seen by a driver or be able to see oncoming traffic) may influence the frequency of deer-vehicle collisions. We used a large spatial window to reduce the influence of flat road surface on estimating slope.
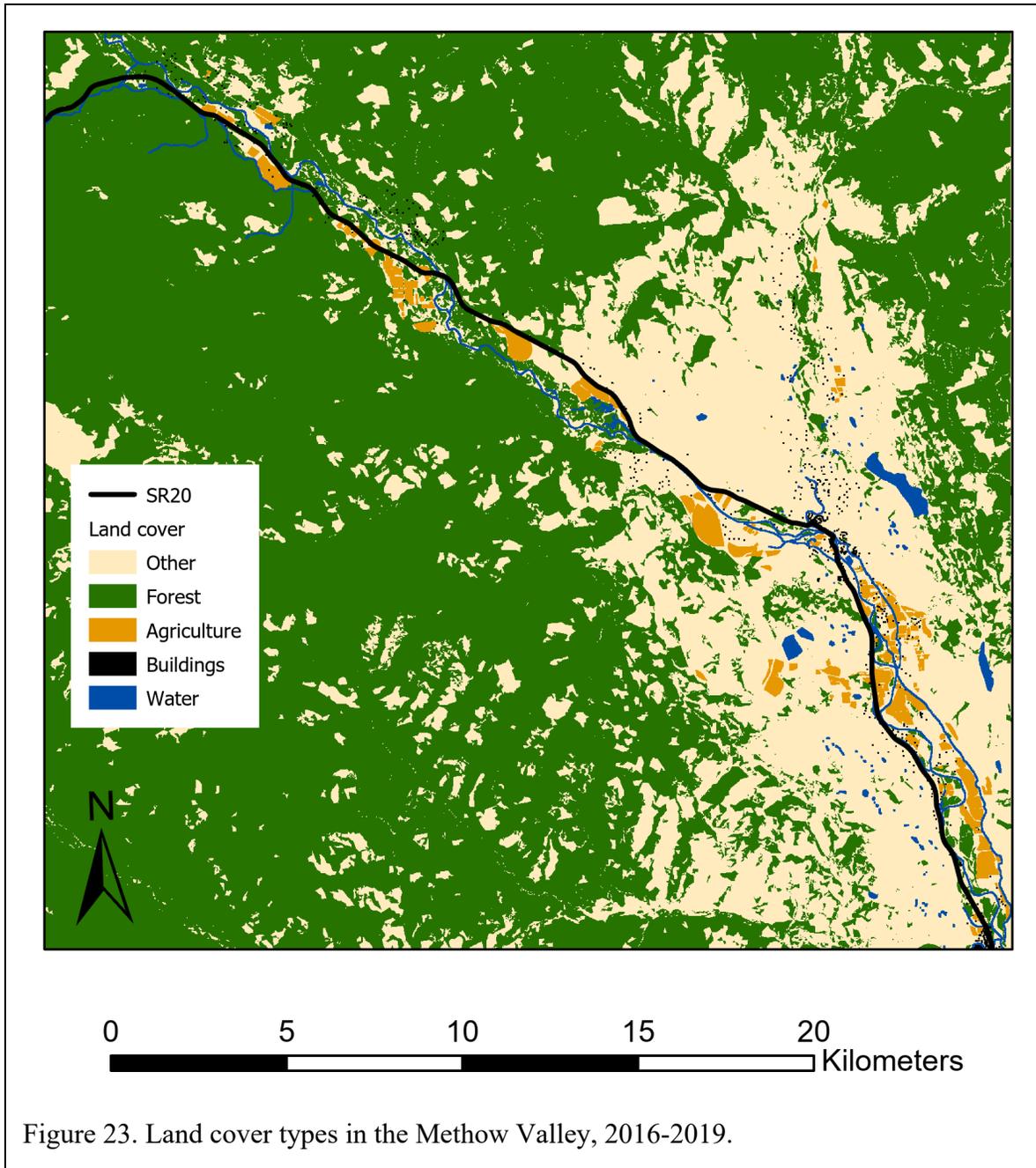
Figure 23. Land cover types in the Methow Valley, 2016-2019.

Road geometry variables

To investigate the role of road geometry in the deer-vehicle collision process, we used sight distance measured and provided by WSDOT. For each segment of road, we assigned the minimum sight distance included in the assessed area as provided by WSDOT, both directions of horizontal as well as vertical (Figure 24). Horizontal sight distance was not provided for areas with 35 mph speed limits and below, these are excluded from this analysis. Areas outside of ARMs where sight distance was measured were given a sight distance of 10000 ft.
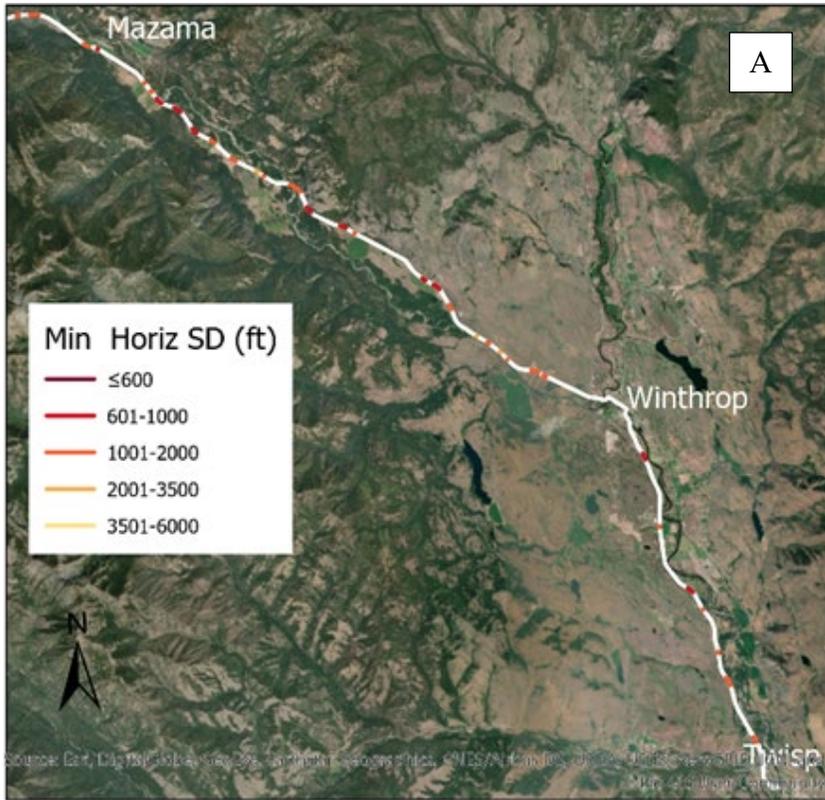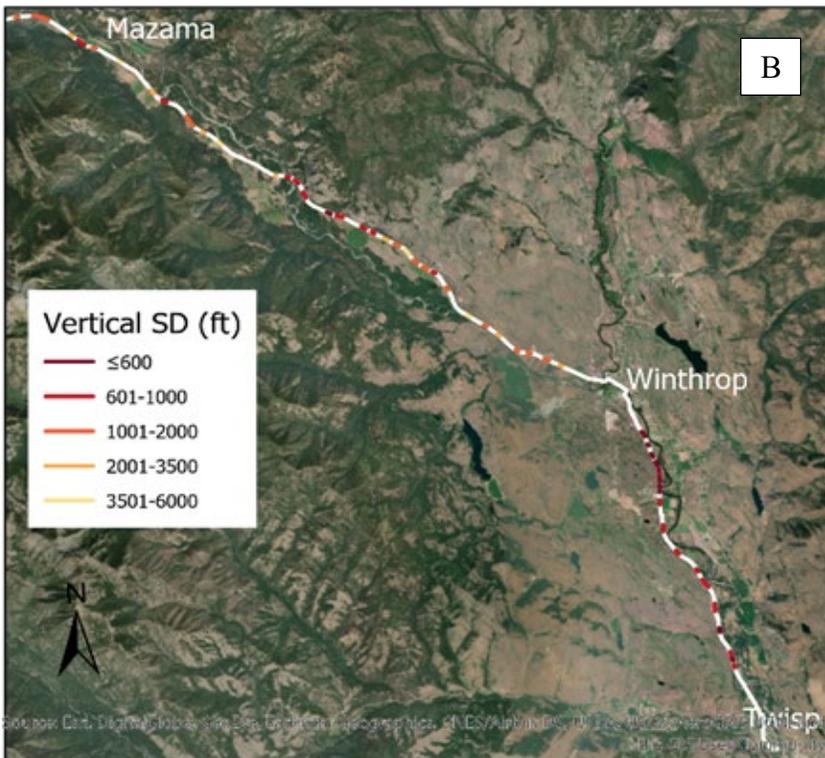
Figure 24. Sight distances along SR 20 in the Methow Valley, Washington, A) Minimum horizontal sight distance, B) Vertical sight distance. White indicates highway segment without measured sight distance limitation.

Modeling Methods

Environmental factors that predict spatially variable frequencies of crossings

We modeled the frequency of deer crossings at each data logger that contained ≥1 deer detections (*n* = 39) to assess what landscape variables were related to frequency of crossings. We standardized the number of detections at each data logger per day by the number of collared deer detected at the logger that day. We note that these data primarily reflect the behavior of mule deer, as the majority of collared animals were resident mule deer.

Models included distance to forest patch, distance to open south facing slope, distance to linear water feature (canal or river, which was correlated with distance to any water feature (r = 0.87) and excluded from further analyses), distance to building, distance to agriculture, whether the nearest agriculture and nearest water were on different sides of the road (0/1), whether the nearest water and nearest open south-facing slope were on different sides of the road (0/1), and whether the nearest open south-facing slope and agriculture were on different sides of the road (0/1). These were analyzed for a set of 18 *a priori* models (Table 1). Frequency of road crossings was natural log-transformed to meet normality assumptions. We used the most parsimonious model with the highest evidence weight to predict the frequency of crossing per deer per day at cameras. We used Akaike's Information Criterion (AIC; Akaike 1973) corrected for small sample size (AICc) and AICc weights for selecting the most parsimonious model (Burnham and Anderson 2002).

Road geometry features that predict frequency of deer-vehicle collisions

To understand whether road geometry features further explained the abundance of deer-vehicle collisions beyond that attributed to deer abundance alone, we modeled the detection-bias corrected estimates of carcass abundance at our camera locations as a proxy for deer-vehicle collisions. We used the camera locations because this is where we could estimate deer abundance. We used a kernel density estimator (ArcGIS Pro 2.4.1, ESRI, Inc.) to create a 10 m resolution raster surface of new carcass density based on carcasses within 1 km (Figure 17). For each camera, this produced an unbiased estimate of abundance, which was log + 0.1 transformed to meet assumptions of normality. We focused on mule deer for these data and associated models because our estimates of abundance were based on frequencies of observed crossings by mule deer, which dominated our sample of radio-collared deer.

We constructed an *a priori* set of 9 linear regression models, each representing various additive and interactive effects of features hypothesized to influence the deer-vehicle collision process. Our null model included deer abundance obtained from the results of the previous modeling (of frequency of crossings). Deer abundance was estimated at each camera associated with its corresponding data logger by dividing the number of images of mule deer or all deer per day by the predicted frequency of deer crossings per day. We used AICc and AICc weights to select the most parsimonious model and determine if and how deer abundance, minimum sight distance (horizontal and vertical), maximum slope within 60 m, and distance to building influenced the abundance of deer-vehicle collisions (Table 2). We used these results to identify linear lengths of

highway where high numbers of deer-vehicle collisions were predicted to occur and refer to these linear lengths as "deer-vehicle collision zones."

Integration of independent carcass and deer-vehicle collision datasets with modeling results

While our linear models were designed to assess environmental and road geometry drivers of the deer-vehicle collision process across the entire study area, finer-scale site-specific application of such models can sometimes lead to spatial scale mismatches and inconsistencies in the reliability of site-specific predictions (Morrison et al. 2006). To improve the utility of our models for site-specific engineering solutions, we heuristically assessed our model predictions against WSDOT's independent carcass and deer collision datasets; this approach was intended to assess site-specificity of our results. For this, we overlaid the deer-vehicle collision zones identified in the previous section onto WSDOT carcass and deer collision data to examine overlap and proximity.

Status of previously identified mule deer migration corridors

To evaluate the status of previously identified mule deer migration corridors, we overlaid current estimates of mule deer abundance and crossings (frequency of photographed encounters) at camera stations onto a georeferenced map of mule deer migration corridors identified by WDFW in the 1980s (Myers et al. 1989). We limited this assessment to the portion of the study area south of mile post 185 (where we identified 7 migration routes documented in the 1980s by Myers et al. (1989)) because our camera data north of mile post 185 were adjusted with movement data from resident deer in the lower elevations south of mile post 185, which limits our most reliable estimates of abundance and associated ability to assess the status of previous migration routes crossing SR 20 to south of mile post 185. We then visually compared where high abundances of mule deer were determined along SR 20 in this study with the migratory routes identified to cross SR 20 in the 1980s and quantified the proportion of previous migration corridors that were active during this study.

Modeling Results

Environmental factors that predict spatially variable frequencies of crossings

The global model fit the dataset of deer crossings reasonably well (Q-Q residual plots), and there was strong evidence that higher frequencies of crossings per deer were positively associated with distance from open south-facing slopes (more crossings farther from these slopes) and negatively associated with distance to linear water feature (canal or river) (more crossings closer to these features; Table 1). The most parsimonious linear model was

$$ln(average\ detections\ per\ deer\ per\ day) = -1.36 + 0.0122 \times \\ distance\ to\ nearest\ south\ facing\ slope\ (m) - 0.00196 \times \\ distance\ to\ nearest\ river\ or\ canal\ (m).$$

Table 1. Linear models of deer crossing frequencies between mile posts 176-201 of SR 20 in the Methow Valley, Washington, January 2018 – October 2018. See text for descriptions of predictors listed under model column. k = number of parameters, AICc = small sample corrected Akaike's Information Criterion, ΔAICc = difference in AICc between model and most parsimonious model, AICc weight = relative model weight according to AICc.

Model (predictors)	k	AICc	ΔAICc	AICc weight
Distance to open south-facing slope + distance to linear water feature	3	156.5	0	0.54
Distance to open south-facing slope + distance to water + located between nearest open south-facing slope and water (0/1)	4	158.3	1.79	0.22
Distance to open south-facing slope	2	159.7	3.15	0.11
Distance to linear water feature	2	162.5	5.97	0.03
Distance to forest + distance to building + distance to agriculture + distance to linear water feature + distance to open south-facing slope	6	162.6	6.06	0.03
Distance to agriculture + distance to linear water feature	3	163.7	7.21	0.01
Distance to nearest building + distance to linear water feature	3	164.9	7.40	0.01
Distance to open south-facing slope + distance to agriculture + located between nearest open south-facing slope and agriculture (0/1)	4	164.0	7.51	0.01
Distance to agriculture + distance to linear water feature + located between nearest agriculture and water (0/1)	4	164.1	7.53	0.01
Distance to nearest forest patch + distance to linear water feature	3	164.7	8.19	0.01
Distance to forest + distance to building + distance to agriculture + distance to linear water feature + distance to open south-facing slope + located between nearest agriculture and water (0/1) + located between nearest open south-facing slope and water (0/1) + located between nearest open south-facing slope and agriculture (0/1)	9	167.0	10.51	0.00
Located between nearest agriculture and water (0/1)	2	168.2	11.70	0.00
Distance to building	2	169.7	13.14	0.00
Located between nearest agriculture and water (0/1) + located between nearest open south-facing slope and water (0/1) + located between nearest open south-facing slope and agriculture (0/1)	4	170.2	13.64	0.00
Located between nearest open south-facing slope and agriculture (0/1)	2	170.6	14.09	0.00
Distance to forest	2	171.2	14.71	0.00
Distance to agriculture	2	172.4	15.92	0.00
Located between nearest open south-facing slope and water (0/1)	2	172.5	16.02	0.00

Road geometry features that predict frequency of deer-vehicle collisions

Our global model of road geometry effects on frequency of deer-vehicle collision fit the new deer carcass abundance data reasonably well (Q-Q residual plots). The frequency of new deer carcasses (as a proxy for deer vehicle collisions) between April 2017 and October 2017 was best explained by an interaction of the abundance of mule deer in the area during that time and the minimum sight distance (vertical or horizontal) at the point in the road, plus the maximum slope within a 60 m buffer (Table 2). The most parsimonious linear model predicted

ln(frequency of deer-vehicle collisions) = 0.09642 + 0.3183 x *predicted mule deer abundance* + 0.0001094 x *minimum sight distance (ft)* – 0.00004199 x *minimum sight distance (ft)* x *predicted mule deer abundance* + 0.05748 x *max slope within 60 m (degrees)*

(Figures 25-27). This same model was also the most parsimonious (highest model weight) in a parallel analysis using all deer (mule and white-tailed deer) combined (Appendix B). A spatially explicit representation of this model revealed nine deer-vehicle collision zones, characterized by linear lengths of highway containing ≥1 0.16-km-segments where relatively high numbers (≥7) of deer-vehicle collisions were predicted to occur during the study period (Figure 27).

Table 2. Linear models of deer-vehicle collision abundances (as represented by new carcasses on the road April 2017 – October 2017) between mile posts 176-201 of SR 20 in the Methow Valley, Washington, April – October 2017. See text for descriptions of predictors listed under model column. *k* = number of parameters, AICc = small sample corrected Akaike's Information Criterion, ΔAICc = difference in AICc between model and the most parsimonious model, AICc weight = relative model weight according to AICc (Burnham and Anderson 2002). Also see Appendix D.

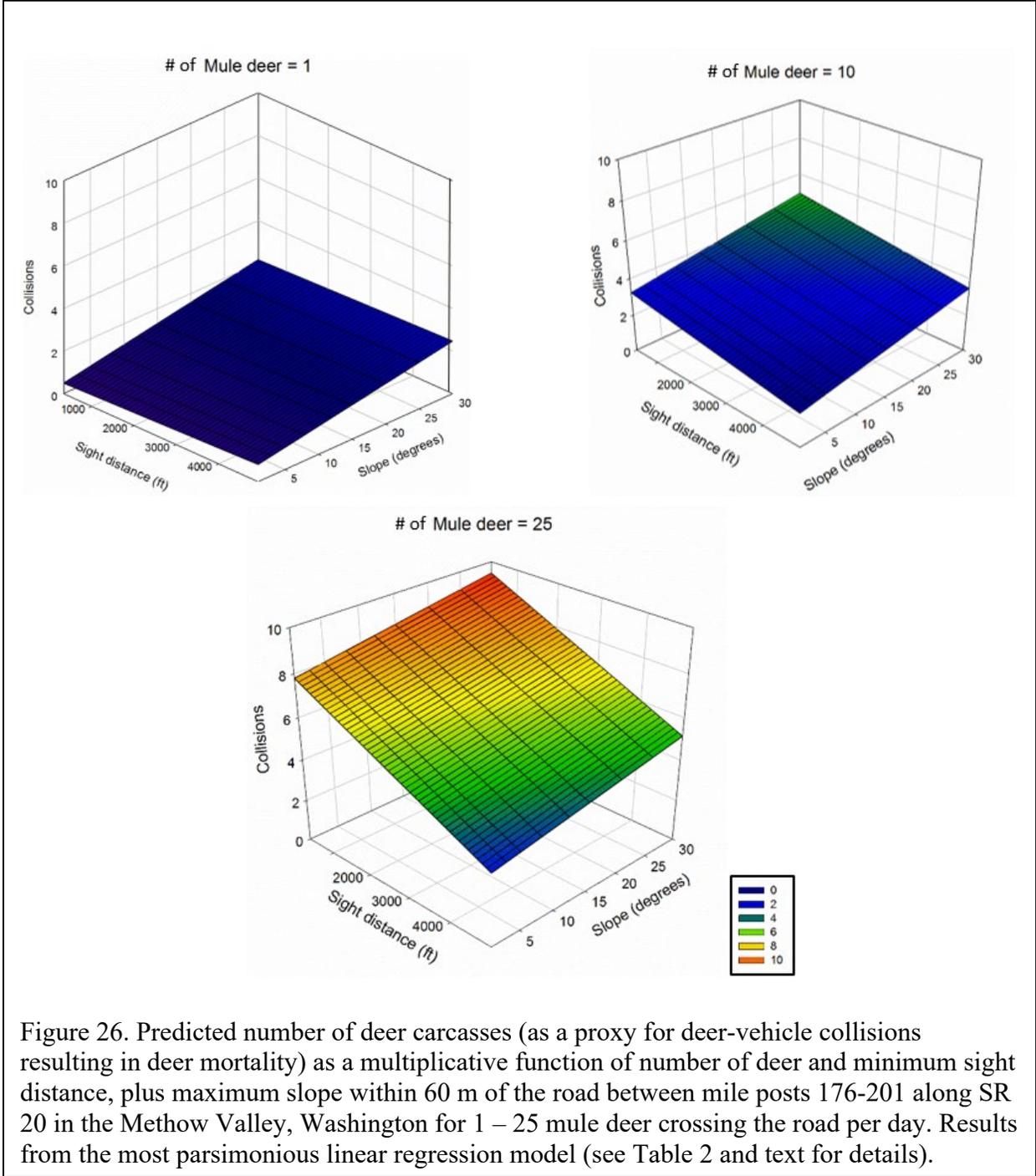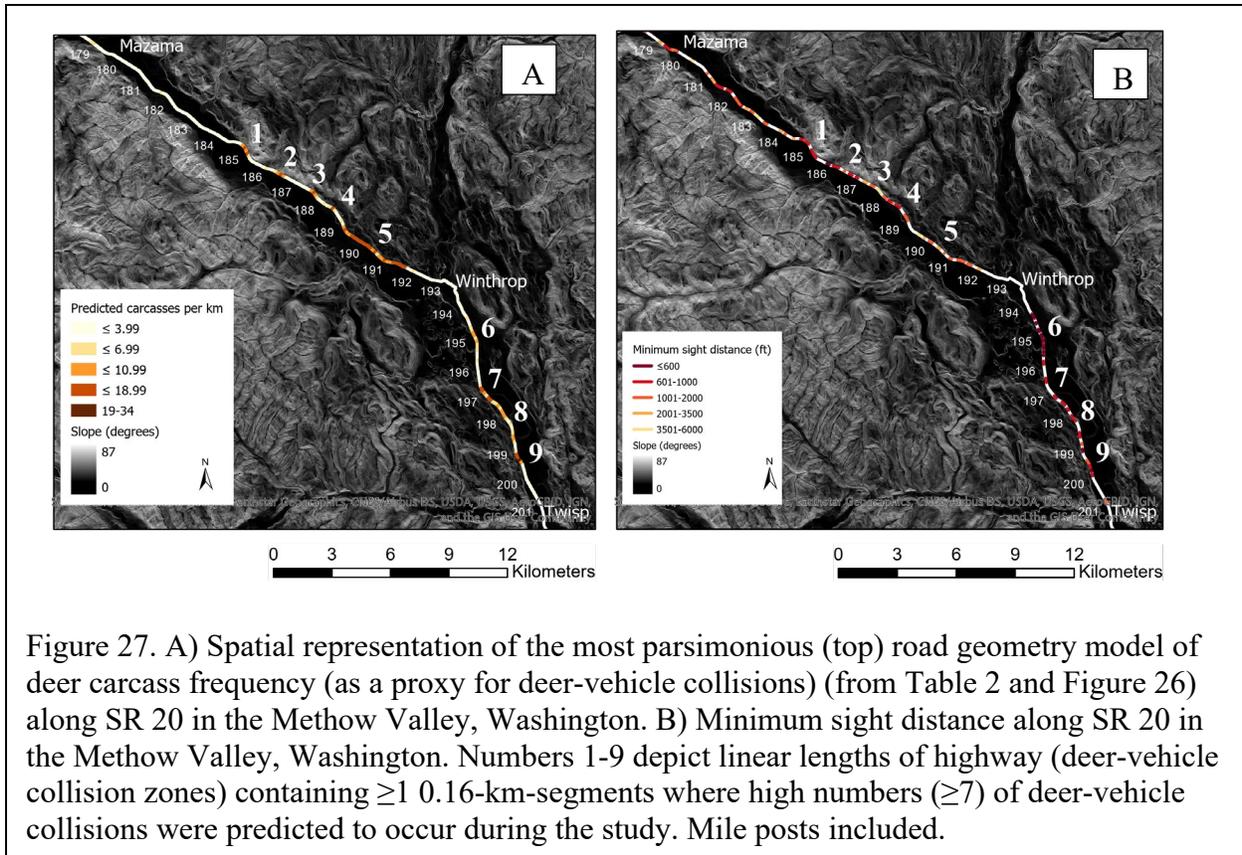| Model (predictors)	*k*	AICc	ΔAICc	AICc weight
Predicted mule deer abundance + minimum sight distance + predicted mule deer abundance*minimum sight distance + maximum slope within 60 m	5	155.7	0.00	0.63
Predicted mule deer abundance + minimum sight distance + predicted mule deer abundance*minimum sight distance + maximum slope within 60 m + distance to building	6	158.0	2.3	0.20
Predicted mule deer abundance + minimum sight distance + predicted mule deer abundance*minimum sight distance	4	159.7	3.91	0.09
Predicted mule deer abundance + maximum slope within 60 m	3	161.1	5.33	0.04
Predicted mule deer abundance + minimum sight distance + predicted mule deer abundance*minimum sight distance + distance to building	4	161.6	5.88	0.03
Predicted mule deer abundance + minimum sight distance	3	165.4	9.64	0.01
Predicted mule deer abundance	2	165.5	9.78	0.00
Minimum sight distance	2	165.9	10.21	0.00
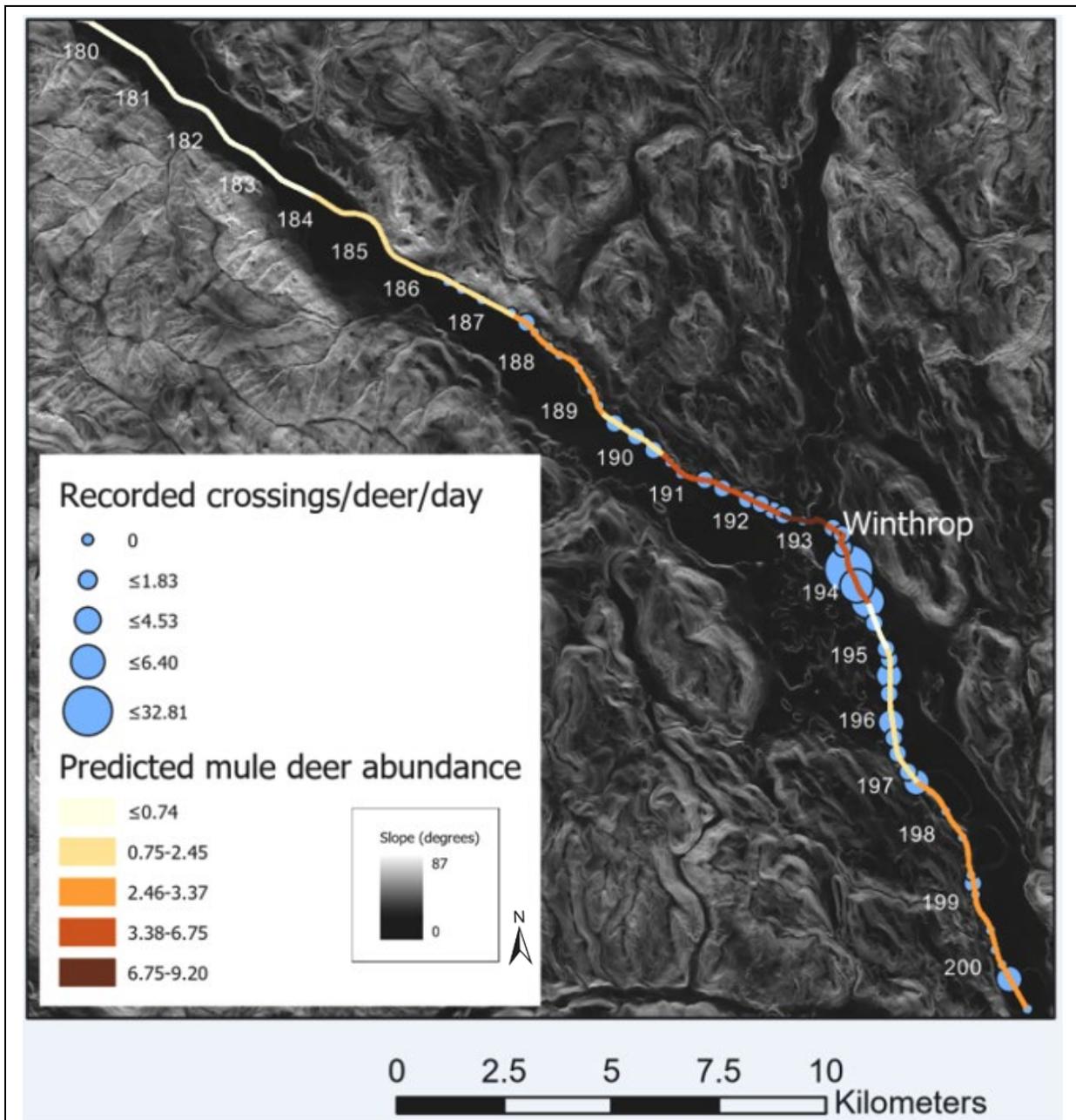
Figure 25. Predicted daily abundance of mule deer that crossed the road (averaged between camera locations by kriging) and the number of times individual (radio-collared) deer crossed the road (based on 49 data loggers) between mile posts 185 – 201 along SR 20 in the Methow Valley, Washington. For example, the abundance of deer crossing SR 20 and the number of times per day they crossed jointly peaked (i.e., high abundance of frequently crossing deer) just south of Winthrop. See text for method used to predict daily mule deer abundance.

Figure 26. Predicted number of deer carcasses (as a proxy for deer-vehicle collisions resulting in deer mortality) as a multiplicative function of number of deer and minimum sight distance, plus maximum slope within 60 m of the road between mile posts 176-201 along SR 20 in the Methow Valley, Washington for 1 – 25 mule deer crossing the road per day. Results from the most parsimonious linear regression model (see Table 2 and text for details).

Figure 27. A) Spatial representation of the most parsimonious (top) road geometry model of deer carcass frequency (as a proxy for deer-vehicle collisions) (from Table 2 and Figure 26) along SR 20 in the Methow Valley, Washington. B) Minimum sight distance along SR 20 in the Methow Valley, Washington. Numbers 1-9 depict linear lengths of highway (deer-vehicle collision zones) containing ≥1 0.16-km-segments where high numbers (≥7) of deer-vehicle collisions were predicted to occur during the study. Mile posts included.

Integration of independent carcass and deer-vehicle collision datasets with modeling results

The assessment of model predictions against the independent WSDOT carcass and deer collision datasets indicated a high level of agreement between them. Additionally, it revealed several areas of SR 20 where deer carcass and collision data were clustered adjacent to 0.16-km-segments of the highway where carcass numbers were predicted to be high (Figure 28).

Status of previously identified mule deer migration corridors

Mule deer in the Methow Valley have been characterized generally as migratory (Myers et al. 1989, Myers et al. 2008, WDFW 2016). Our study focused on the peak period of mule deer-vehicle collisions and carcass removals (May-October). Based on winter trapping, radio-tracking
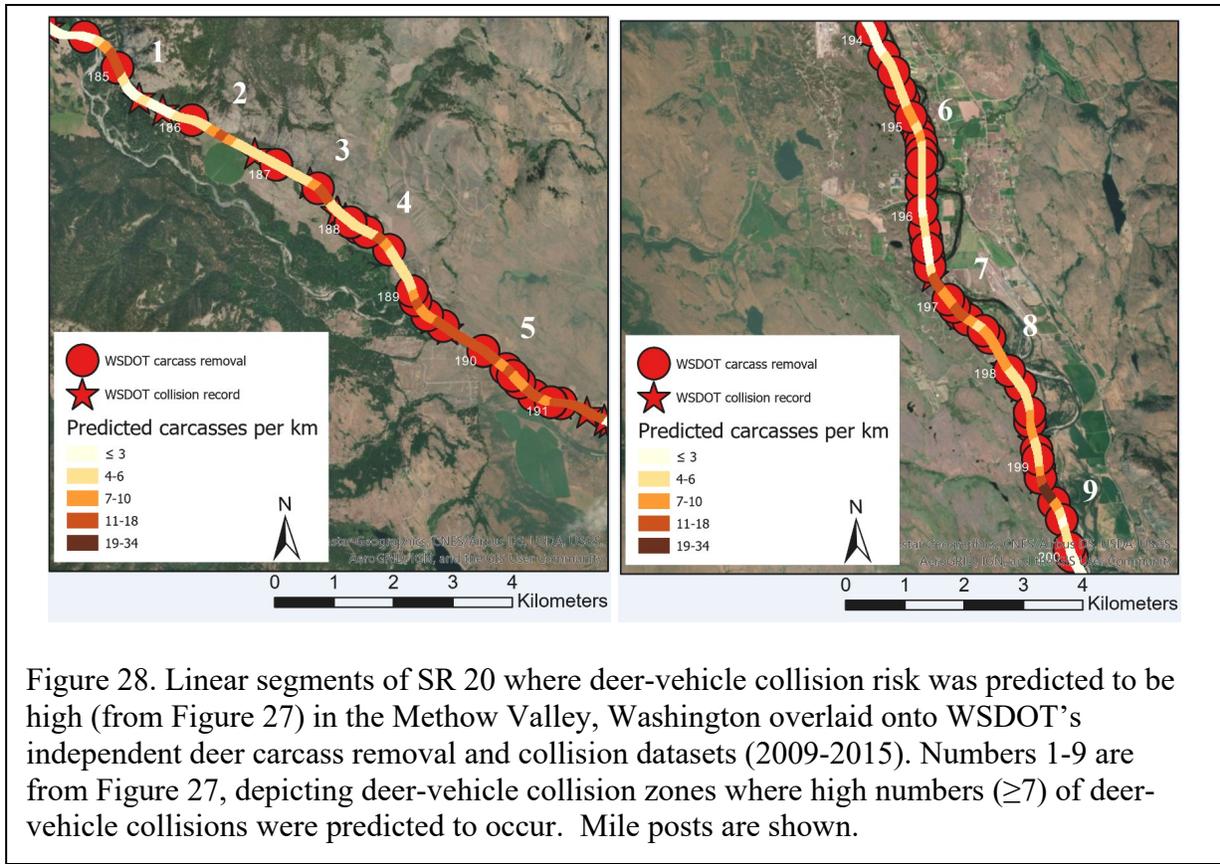
Figure 28. Linear segments of SR 20 where deer-vehicle collision risk was predicted to be high (from Figure 27) in the Methow Valley, Washington overlaid onto WSDOT's independent deer carcass removal and collision datasets (2009-2015). Numbers 1-9 are from Figure 27, depicting deer-vehicle collision zones where high numbers (≥7) of deer-vehicle collisions were predicted to occur. Mile posts are shown.

during the peak period of deer-vehicle collisions (May-October), and data loggers, we classified 68% ($n = 15$) of the 22 does radio-collared along SR 20 as non-migratory, year-round residents with home ranges that straddled SR 20. Despite using recorded numbers of deer photos in combination with the frequency of crossings by individual collared deer to estimate spatially explicit estimates of deer abundance, deep snows north of mile post 185 during winter trapping led to an absence of deer to capture and collar in that northern region of the study area. Additionally, we also did not detect any of our collared deer north of mile post 185 the following summer, further indicating that our sample of collared deer exhibited strong year-round site fidelity and space use patterns that may diverge from those of deer that migrate through the area. Despite our pilot study revealing that increased abundance corresponds with increased numbers of crossings (Figure 13), our camera data north of mile post 185 were adjusted with movement data from resident deer in the lower elevations south of mile post 185, which limits our most reliable estimates of abundance and associated ability to assess the status of previous migration routes crossing SR 20 to south of mile post 185. Focusing on the region between mile posts 185-201, we found that 100% ($n = 7$) of the locations in this region where deer migration routes crossed SR 20 in the 1980s were active during this study (Figure 29A and B).

Figure 29. Status of past mule deer migratory corridors; (A) predicted mule deer abundance and (B) average number of mule deer photos overlaid onto mule deer movement corridors (bold lines) identified in the 1980s (Meyers et al. 1989). Mile posts are shown.
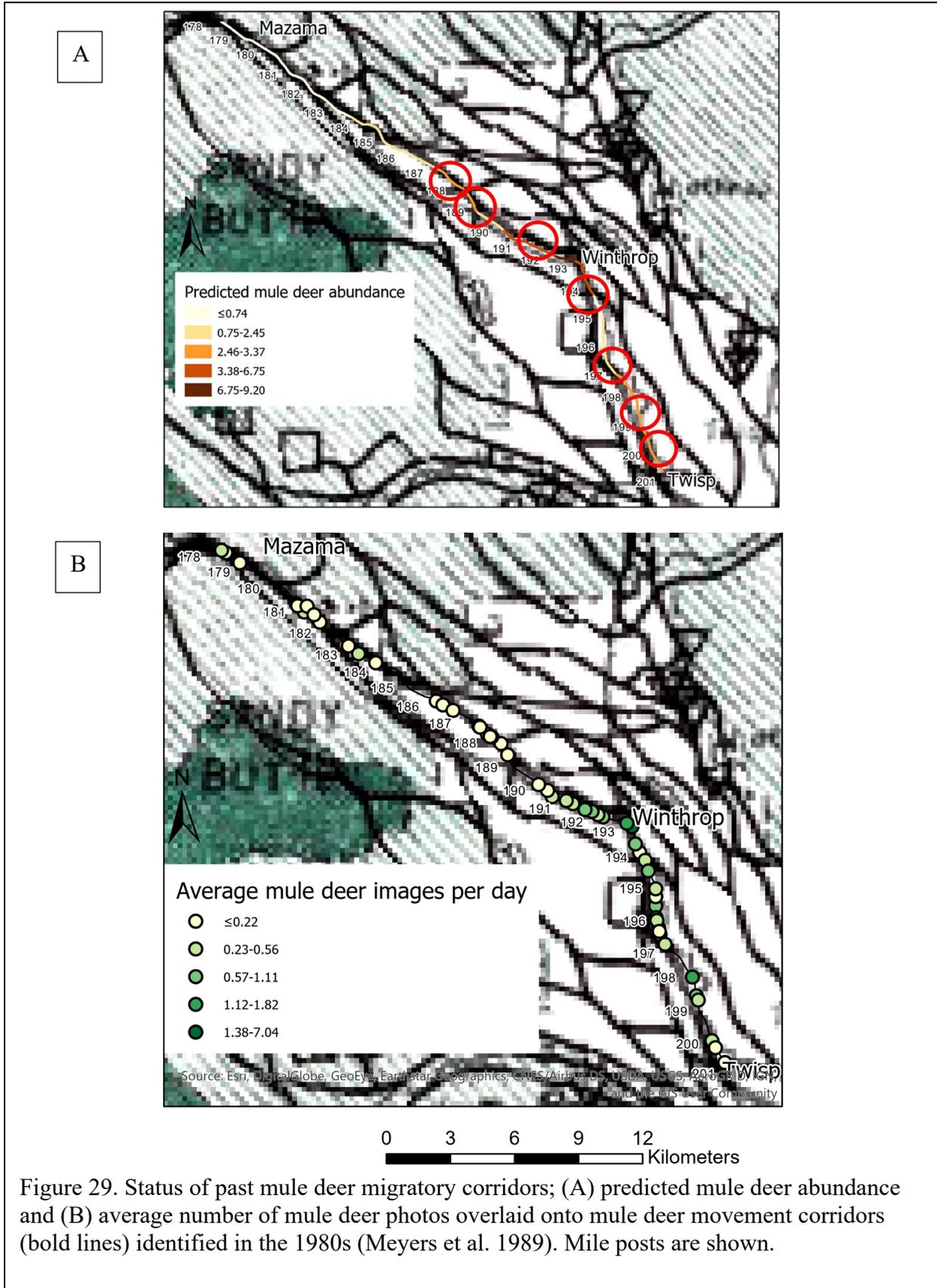
DISCUSSION

The majority (68%) of collared deer sampled during this study were non-migratory, year-round residents with home ranges that straddled SR 20. This finding differs from what others previously found in the valley—that mule deer were primarily migratory (Myers et al. 1989, Myers et al. 2008, WDFW 2016); this life history strategy is more common in areas where variable precipitation and snow cover occurs (e.g., southern California; Nicholson et al. 1997). This pattern, where approximately three quarters of sampled female deer exhibited a non-migratory life strategy, is not commonly reported in northern ungulate populations because migration to lower elevations during winter is necessary for animals to survive deep snow associated with northern winters (Sawyer et al. 2005, Hebblewhite and Merrill 2009, Manning 2010, Anderson et al. 2012, Manning and Garton 2012, Middleton et al. 2013, WDFW 2016). Migration also enables northern ungulates to access highly nutritious forage in high-elevation spring and summer ranges and minimize energy expenditure in shallow snow depths within winter ranges, which are linked to fecundity and survival (Cook et al. 2004, Pettorelli et al. 2007, Tollefson et al. 2010). The high proportion of non-migratory resident mule deer we found is in line with descriptions from local residents who reported an increase in the number of deer in the valley over the past 50 years, and that deer were essentially non-existent prior to that time except for small isolated areas like the area southwest of Winthrop identified by Myers et al. (1989). In combination with these reports, our findings suggest a growing population segment of non-migratory mule deer around and south of the town of Winthrop.

The positive correlation between probability of crossings and number of live deer and the significant effect of deer numbers on frequency of crossings (Figure 12-14) were expected, and indicate that the frequency of highway crossings by deer is a meaningful metric to investigate the deer-vehicle collision process. Mule deer abundance and frequency of road crossings were particularly concentrated around the town of Winthrop (Figures 20 and 25), indicating that the juxtaposition of this location within the regional migratory pathways may play an important role, among other factors, in the abundance of deer in this area. The confluence of the Methow and Big Valleys is characterized by open, low-elevation flats and hillsides, access to forage and water (river and canals), and south-southwest facing slopes, consistent with winter habitat preferences of mule deer elsewhere in the northwest (Manning 2010, WDFW 2016). The elevation of this area is lower than the surrounding summer range and at the upper elevation range of suitable mule deer winter habitat, providing shallower snow depths in winter for deer to navigate. High incidence of solar radiation on open south-facing slopes, coupled with prevailing winds from the northwest, provide deer with reduced snow depths compared to neighboring forested slopes or flat land aids, and offer thermal protection and more easily accessible forage. Deer also exhibited an increase in road crossing in areas closer to rivers and canals—potentially because flowing waters present in these linear water features freezes later and thaws earlier than water impoundments. Although not important in our models, the presence of agriculture close to towns in the study area may also contribute to the prevalence of year-round, resident deer present near Winthrop because highly nutritious agricultural crops (e.g., winter wheat) have been linked to increased deer body condition, survival, and spatial shifts (WDFW 2016) – potentially changing space use and/or altering migration behavior.

After accounting for deer abundance in our models, we found that the number of deer-vehicle collisions was directly related to minimum sight distance by vehicle drivers and the maximum slope occurring within 60 m from the road. Sight distance corresponds to a vehicle's driver's ability to detect a deer. Our best model predicted that deer-vehicle collisions decreased with increasing sight distance. We also found that deer-vehicle collisions increased with increasing slope and abundance of deer crossing the road. When deer numbers were low, we found a smaller influence of sight distance on deer-vehicle collisions, with steep slopes near the road having a greater negative impact. This may be due to the speed and momentum of deer entering the roadway as they came down from above, reducing the reaction time of deer and drivers in those situations. The effect of sight distance on collisions increased with increasing deer numbers, with a strong effect at locations where high numbers of mule deer per day occurred (e.g., near the town of Winthrop). However, speed limit likely attenuated the relationship between deer numbers and deer-vehicle collisions in and around the town of Winthrop (between mile posts 192 and 195), which resulted in the absence of a deer-vehicle collision zone in this area despite high deer numbers.

Because resident deer, which navigate traffic daily, may behave and interact differently with highways compared to migratory deer, a more thorough understanding of the migratory status is needed. Mule deer in the Methow Valley continue to use previously recorded migration routes (Figure 29). We detected this despite using crossing data largely from resident deer to adjust the numbers of deer photos – this was the case probably because the number of photos increased in areas where the number of deer crossing the road included migrants. This finding was not surprising given that mule deer exhibit strong fidelity to migratory routes throughout their range (e.g., Sawyer et al. 2013). In addition to documenting the continued use of traditional migration routes, this study revealed additional locations along the highway where high abundances and frequencies of crossings occur, depicting a combination of migration routes for migratory animals and local movement routes used by resident deer. Future studies could involve sampling both migrant and resident deer to determine the contributions of each segment within this deer population in deer-vehicle collisions. Efforts to reduce deer-vehicle collisions may differ depending on which segment of the population is targeted for engineering solutions.

RECOMMENDATIONS

As most of the radio-collared deer during this study were year-round resident mule deer, the following recommendations are based primarily on the movements of resident deer in the Methow Valley. These resident mule deer appear to constitute the majority of deer in areas where most collisions and carcass removals occurred (i.e., from mile 190 to 198). We note that the recommended solutions below may not take into account specific management goals established by resource agencies for migratory deer populations in the region or those focused on white-tailed deer.

To identify and recommend zones along SR 20 where engineering solutions can be applied to reduce deer-vehicle collisions, we began by improving the specificity of our model results. To accomplish this, we extended deer-vehicle collision zones (from Figures 27 and 28) out by 0.16-km increments in both directions to encompass contiguous highway increments that contained a WSDOT-documented carcass or collision. We excluded carcasses on mile posts because

WSDOT's records were linked to the nearest mile post in some cases (Figure 30). This resulted in nine zones for recommending engineering solutions (between mile posts 184-200; Figure 30). Despite a high abundance of likely resident deer in and around the town of Winthrop (between mile posts 192 and 194), low numbers of carcasses and deer-vehicle collisions led to this area not being identified as a recommended zone for engineering solutions.

Lengths of recommended engineering zones ranged from 0.48-4.32 km (Table 3); the lengths of three zones (1-3) were comprised entirely of deer-vehicle collision zones, and the remaining six were comprised of both deer-vehicle collision zones and extensions. Engineering solutions carried out in the more northern zones (1-4) would benefit white-tailed deer, which dominate deer numbers in this area of the study area. Zones 5-7 would benefit both white-tailed and mule deer, with increasing benefits to mule deer in zones 6 and 7. Zones 8 and 9 would primarily benefit mule deer, which dominate deer numbers there.

Because the implementation of engineering solutions would likely take place over time, we developed two methods to prioritize the implementation of engineering solutions among these nine zones according. These include: 1) the percent reduction in overall deer-vehicle collision numbers along this stretch of highway (Figure 31) and 2) a biological benefit to local deer herds based on the proportion of mule deer mortality (or loss of animals) due to deer-vehicle collisions relative to the corresponding local herd size (Figure 32). This latter ranking metric is grounded in the recognition that high mortality in local deer groups could lead to reductions in local deer abundance and familial (genetic) lineages, and that the conservation of local deer groups scales up to improved health of regional deer herds. It is provided here to provide a biological context for prioritizing zones for engineering solutions.

Zone 5 just north of Winthrop was the top ranked zone, containing the highest percentage of deer carcasses and collisions (Table 3). Implementation of engineering solutions that prevent deer-vehicle collisions in this zone would reduce the total annual number of deer-vehicle collisions between the towns of Mazama and Twisp by 18.6%. This zone is also ranked as a high priority for biological importance for white-tailed and mule deer. As such, we recommend zone 5 as a top priority for implementing engineering solutions.

Our second recommended priority for engineering solutions is zone 6 due to the high percentage of deer-vehicle collisions (11.9%) combined with the highest ranking for biological importance (Table 3), with an estimated 14% loss of local deer abundance attributed to deer-vehicle collisions. Engineering solution in this zone would benefit both species. This is closely followed by our third recommended zone (zone 9), which would primarily benefit mule deer and has 12.6% of deer-vehicle collisions but ranked only 6th in biological importance. Our fourth recommended zone for engineering solutions is zone 7, with benefits to both species and 8.7% of deer-vehicle collisions, with the 3rd highest ranking for biological importance. Engineering solutions implemented in these four zones (5, 6, 7, and 9) would result in a 51.9% cumulative reduction in deer-vehicle collisions annually between the towns of Mazama and Twisp. Engineering solutions implemented in all 9 zones would result in a 57.8% reduction in deer-vehicle collisions between Mazama and Twisp.

Recognizing that recommendations of site-specific engineering solutions is beyond our expertise and the project scope, we provide the following general description of potential technologies and engineering solutions. Various technologies have been developed to reduce wildlife-vehicle collisions across North America. Laser detection systems and roadside animal activated detection systems (e.g., Grace et al. 2017) continue to be developed and tested. Laser detection systems that can activate warning signs could prove helpful. Reduced speed limits and deer reflectors are common, but each has its own strength and drawback (e.g., https://www.wsdot.wa.gov/environment/protecting/wildlife-collisions). For example, reduced speed limits may help reduce wildlife-vehicle collisions, but passing, tailgating, and speeding may arise where drivers perceive unreasonably low speed limits, and enforcement can be difficult. However, we deduce that the reduced speed limit ($\leq$35mph) in and around the town of Winthrop (between mile posts 192 and 195) likely contributed to a low number of deer-vehicle collisions despite high deer numbers, indicating that reduced speed limits may provide a functional solution in some areas of SR 20. Our models indicate that increasing sight distance reduces deer-vehicle collisions, and increasing the minimum vertical sight distance in areas like zone 6 (currently 220 ft; Table 3) would help reduce collisions.

Highway crossing structures (wildlife over- and under-passes) constructed in British Columbia's National Parks, Montana highways, and along Interstate 90 in Washington State by WSDOT have shown marked success at reducing wildlife-vehicle collisions and contributing to local and regional wildlife populations. Interlinking multiple wildlife crossing structures with wildlife-proof fencing on both sides of a highway can reduce wildlife-vehicle collisions along stretches of highways. At 4.32 km long, zone 5 contains various sites along its length where over- and under-passes could be engineered and linked by deer-proof fencing on both sides of the highway. To reduce deer from walking around the ends of fencing, cattle guards extending across the road at each end of the zone could be considered.
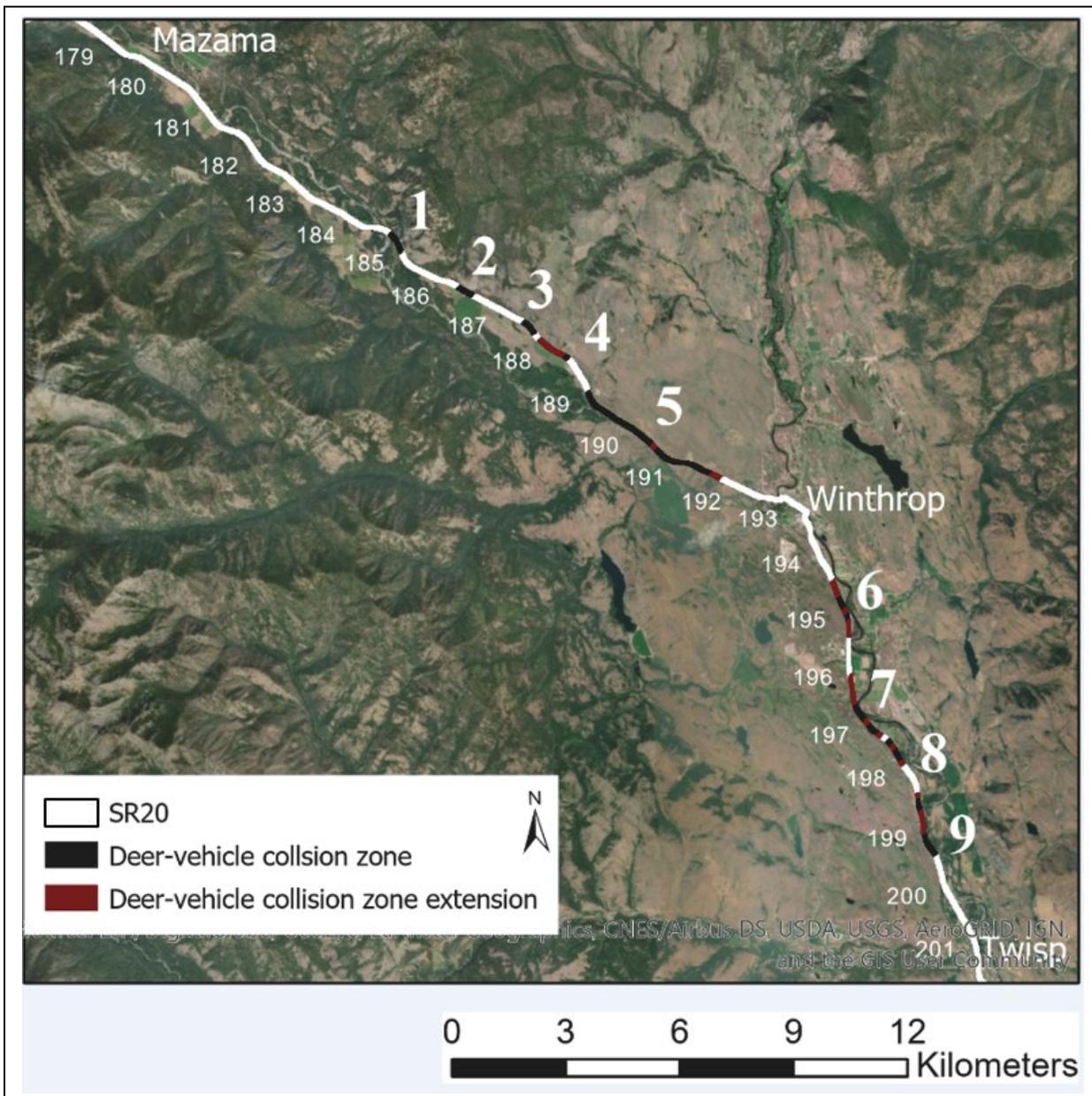
Figure 30. Recommended zones for engineering solutions (comprised of both deer-vehicle collision zones and zone extensions) between SR 20 mile posts 176-201 in the Methow Valley, Washington. Numbers 1-9 correspond to deer-vehicle collision zones presented in Figure 27; zones were not identified north of mile post 184. Zone extensions derived from extending existing zones into adjacent clusters of independent WSDOT carcasses and deer-vehicle collision records. Mile posts included.

Table 3. Characteristics and ranking of recommended zones for engineering solutions between mile posts 178-201 in the Methow Valley, Washington. Zones are labeled 1-9 from north to south.

Zone	Coordinates at north-end[1] Northing	Easting	Linear length (km)	Model output[2]	Percent of length Carcass/ collision data[3]	Minimum sight distance[4] (ft)	Target species[5]	Ranking by deer-vehicle collisions[6]	Ranking by biological importance[7]
1	5380199	697612	0.64	100	0	650 V	WTDE	8 (0.3)	8
2	5378775	699398	0.48	100	0	875 V	WTDE	9 (0.0)	7
3	5377855	701116	0.48	100	0	4,491 V	WTDE	7 (0.4)	9
4	5377403	701544	0.96	16	84	799 V	WTDE	5 (4.6)	5
5	5376044	702834	4.32	89	11	1,058 H	BOTH	1 (18.6)	2
6	5371052	709279	1.60	30	70	220 V	BOTH	3 (11.9)	1
7	5368570	709750	1.92	42	58	668 V	BOTH	4 (8.7)	3
8	5366839	710720	0.80	60	40	739 H	MUDE	6 (0.6)	4
9	5365464	711521	1.76	55	45	902 V	MUDE	2 (12.6)	6

[1] NAD83, Zone 10.

[2] From road geometry model; see Figures 26 and 27 and Table 2.

[3] From WSDOT carcass data from 2009 to 2015 independent of the road geometry model.

[4] V = vertical sight distance, H = horizontal sight distance (whichever was shorter).

[5] WTDE = white-tailed deer, MUDE = mule deer, BOTH = both deer species.

[6] Determined from the percentage of deer-vehicle collisions (number of carcasses and deer-vehicle collisions during a given year / total number between SR 20 mile posts 178-201 during that year) averaged over 7 years (2009-2015). Average percentages in parentheses. Ranking ranges from 1-9, with 1 being highest. Carcass and collision data from WSDOT.

[7] Determined from the proportion of deer mortality (number of carcasses relative to local abundance of mule deer) predicted along SR 20 between April and October during the study period (see text for details). Ranking ranges from 1-9, with 1 being most biologically important (i.e., engineering solutions in this zone would reduce the greatest proportional loss (attributed to deer-vehicle collisions) to the local deer herd).
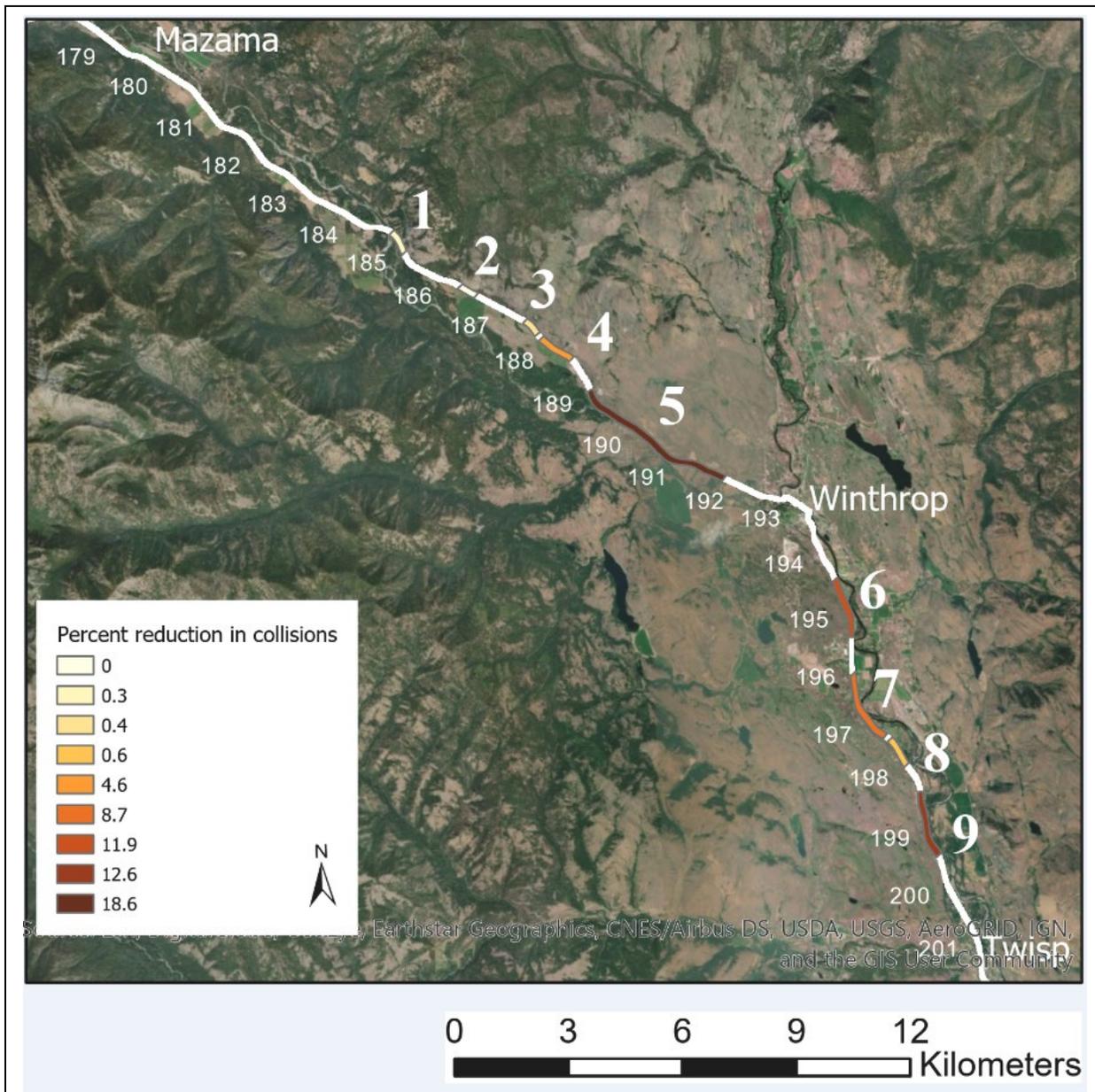
Figure 31. Pertentage of deer-vehicle collisions in each of 9 recommended zones for engineering solutions between SR 20 mile posts 178-201 in the Methow Valley, Washington. Percentage calculated as the number of carcasses and deer-vehicle collisions during a given year / total number across the study area during that year) averaged over 7 years (2009-2015). Carcass and collision data from WSDOT. Numbers 1-9 are from Figure 27, depicting predicted deer-vehicle collision zones. Mile posts included.

Figure 32. Proportion of mule deer mortality (number of carcasses relative to local mule deer abundance) predicted along SR 20 between April and October (i.e., detection bias-corrected estimate of carcass abundance / estimated mule deer abundance x 180 days) between mile posts 178-201 along SR 20 in the Methow Valley, Washington. Numbers 1-9 are from Figure 27, depicting deer-vehicle collision zones where high numbers (≥7) of deer-vehicle collisions were predicted to occur. Mile posts included.

ACKNOWLEDGMENTS

LITERATURE CITED

Akaike, H. 1973. Information theory and an extension of the maximum likelihood principle. In B. N. Petrov & F. Caski (Eds.). Proceedings of the Second International Symposium on Information Theory (pp. 267–281). Budapest, Akademiai Kiado.

Anderson, E.D., R.A. Long, M.P. Atwood, J.G. Kie, T.R. Thomas, P. Zager, and R.T. Bowyer. 2012. Winter resource selection by female mule deer Odocoileus hemionus: functional response to spatio-temporal changes in habitat. Wildlife Biology, 182: 153–163.

Bissonette, J. A. 2002. Scaling roads and wildlife: the Cinderella Principle. Zeitschrift fur Jagdwissenschaft, Supplement 48:208–214.

Burnham, K. P. and D. R. Anderson. 2002. Model Selection and Multimodel Inference: A Practical Information-Theoretic Approach. Springer.

Casady, D.S. and M.L. Allen. 2013. Handling adjustments to reduce chemical capture-related mortality in black-tailed deer. California Fish and Game 99:104-109.

Clover, M. R. 1954. A portable deer trap and catch-net. California Fish and Game 40: 367-373.

Clover, M. R. 1956. Single-gate deer trap. California Fish and Game 42: 199-210.

Cook, J.G., B.K. Johnson, R.C. Cook, R.A. Riggs, T. Delcurto, L.D. Bryant, and L.L. Irwin. 2004. Effects of summer-autumn nutrition and parturition date on reproduction and survival of elk. Wildlife Monographs 155:1–61.

Grace, M.K., D.J. Smith, and R.F. Noss. 2017. Reducing the threat of wildlife-vehicle collisions during peak tourism periods using a Roadside Animal Detection System. Accident Analysis and Prevention 109:55-61.

Hebblewhite, M., and E.H. Merrill. 2009. Trade-offs between predation risk and forage differ between migrant strategies in a migratory ungulate. Ecology, 90: 3445–3454.

Homer, C.G., Dewitz, J.A., Yang, L., Jin, S., Danielson, P., Xian, G., Coulston, J., Herold, N.D., Wickham, J.D., and Megown, K. 2015. Completion of the 2011 National Land Cover Database for the conterminous United States-Representing a decade of land cover change information. Photogrammetric Engineering and Remote Sensing, v. 81, no. 5, p. 345-354.

Manning, J.A. 2010. Population dynamics of rocky mountain elk and mule deer: competition, habitat selection, wolf predation, and predictions under climate change. Ph.D. dissertation. University of Idaho.

Manning, J.A. and E.O. Garton. 2012. Reconstructing historical snow depth surfaces to evaluate changes in critical demographic rats and habitat components of snow-dependent and snow-restricted species. Methods in Ecology and Evolution 3:71-80.

Morrison, M.L., B. Marcot, and W. Mannan. 2006. Wildlife-habitat relationships: concepts and applications. 3rd Ed. Island Press, Washington DC. 493p.

Myers, W. L., R. H. Naney, and K. R. Dixon. 1989. Seasonal movements and home ranges of female mule deer in western Okanogan County, Washington. Washington Department of Wildlife P-R Completion Report W-95-R. 34p.

Myers, W. L., W. Y. Chang, S. S. Germaine, W. M. Vander Haegen, and T. E. Owens. 2008. An analysis of deer and elk-vehicle collision sites along state highways in Washington State. Completion Report, Washington Department of Fish and Wildlife. Olympia, WA 40p.

McClintock, B.T., White, G.C., Antolin, M.F. and Tripp, A.D. 2009. Estimating abundance using mark-resight when sampling is with replacement or the number of marked individuals is unknown. Biometrics, 65, 237–246.

Middleton, A.D., M.J. Kauffman, D.E. McWhirter, J.G. Cook, R.C. Cook, A.A. Nelson, M.D. Jimenez, and W.D. Klaver. 2013. Animal migration amid shifting patterns of phenology and predation: lessons from a Yellowstone elk herd. Ecology, 94: 1245–1256.

Nicholson, M.C., R.T. Bowyer, and J.G. Kie. 1997. Habitat selection and survival of mule deer: tradeoffs associated with migration. Journal of Mammalogy 78: 483–504

Pettorelli, N., F. Pelletier, Von, A. Hardenberg, M. Festa-Bianchet, and S.D. Côté. 2007. Early onset of vegetation growth vs. rapid green-up: impacts on juvenile mountain ungulates. Ecology, 88: 381–390.

Sawyer, H., F. Lindzey, and D. McWhirter. 2005. Mule deer and pronghorn migration in western Wyoming. Wildlife Society Bulletin 33: 1266–1273

Sawyer, H., M. J. Kauffman, A. D. Middleton, T. A. Morrison, R. M. Nielson, & T. B. Wyckoff. 2013. A framework for understanding semi-permeable barrier effects on migratory ungulates. Journal of Applied Ecology 50:68-78.

Thompson, M.J., R.E. Henderson, T.O. Lemke, and B.A. Sterling. 1989. Evaluation of a collapsible Clover trap for elk. Wildlife Society Bulletin 17:287-290.

Tollefson, T.N., L.A. Shipley, W.L. Myers, D.H. Keisler, and D. Nairanjana. 2010. Influence of summer and autumn nutrition on body condition and reproduction in lactating mule deer. Journal of Wildlife Management 74: 974-986.

USGS. 2011. U.S. Geological Survey Gap Analysis Program, 20160513, GAP/LANDFIRE National Terrestrial Ecosystems. https://doi.org/10.5066/F7ZS2TM0

VerCauteren, K.C., J. Beringer, and S.E. Hygstrom. 1999. Use of netted cage traps for capturing white-tailed deer. USDA National Wildlife Research Center - Staff Publications. 833. https://digitalcommons.unl.edu/icwdm_usdanwrc/833.

Washington Department of Fish and Wildlife. 2016. Washington State Mule Deer Management Plan, Wildlife Program, Washington Department of Fish and Wildlife, Olympia, WA, USA. 144 p.

Zeigler, D. L. 1978. The Okanogan mule deer. Biological Bulletin No.15. Washington Department of Game, Olympia, WA, USA. 106 p.

Appendix A. Photographs recorded by 59 game cameras along State Route 20 between mile posts 176-201 in the Methow Valley, Washington, April-October 2017.

Camera	Mule deer	Unk deer	White-tailed deer	Both deer	Bird	Black bear	Cougar	Coyote	Chipmunk	Domestics	Human	Marmot	Moose	Mouse	Raccoon	Squirrel
BTC DOE 01	35	18	0	0	0	0	0	19	0	23	40	0	0	0	0	0
BTC DOE 02	47	4	8	0	0	0	0	0	0	0	5	0	0	0	0	0
BTC DOE 03	34	18	17	0	0	0	0	0	0	0	21	0	0	0	0	0
BTC DOE 04	22	3	0	0	2	0	0	0	0	0	15	0	0	0	1	0
BTC DOE 05	78	19	0	0	2	0	0	1	0	1	8	0	0	0	0	0
BTC DOE 06	206	23	0	0	1	0	0	9	0	14	4	0	0	0	0	0
BTC DOE 07	33	24	2	0	42	0	0	0	0	0	9	0	0	0	0	0
BTC DOE 08	26	14	0	0	2	0	0	0	0	3	6	0	0	1	0	0
BTC DOE 09	31	1	4	0	34	0	0	0	0	0	10	0	0	0	0	1
BTC DOE 10	163	22	0	0	14	0	0	0	0	0	41	0	0	0	1	0
BTC DOE 11	1310	10	0	0	17	0	0	0	0	11	15	0	0	0	32	3
BTC DOE 13	278	96	0	0	59	0	0	0	0	31	14	0	0	0	0	0
BTC DOE 14	124	5	59	1	6	0	0	0	0	1	4	0	0	0	0	1
BTC DOE 15	77	37	60	0	1	0	0	0	0	227	3	0	0	0	0	0
BTC DOE 16	199	57	59	0	1	0	0	1	0	0	6	0	0	0	0	0
BTC DOE 17	168	139	189	1	68	0	0	0	0	0	902	0	2	0	0	0
BTC DOE 18	94	86	196	0	0	0	0	2	0	2	6	0	0	0	0	0
BTC DOE 19	91	110	29	0	0	3	0	1	0	1	92	0	0	0	0	0
BTC DOE 20	51	31	10	0	1	0	0	1	0	1	49	0	0	0	0	0
BTC DOE 21	6	4	0	0	11	0	0	0	0	1	5	0	0	0	0	0
BTC DOE 22	23	6	2	0	0	0	0	0	0	0	11	0	0	0	0	0
BTC DOE 23	31	23	7	0	182	0	0	0	0	0	6	0	0	0	0	0
BTC DOE 24	41	15	16	0	1	0	0	1	0	0	26	0	0	0	0	0
BTC DOE 25	0	0	0	0	0	0	0	0	0	0	3	0	0	0	0	0
BTC DOE 26	4	0	25	0	0	1	0	1	0	0	8	0	0	0	0	0
BTC DOE 27	29	28	6	0	1	1	0	0	0	0	9	0	0	5	0	0
BTC DOE 28	40	52	72	0	8	0	0	0	0	17	5	0	0	0	0	0
BTC DOE 29	25	4	20	0	7	0	0	0	0	0	1	0	0	0	0	0
BTC DOE 30	9	2	6	0	1	0	0	2	0	0	6	0	0	0	0	0
WSDOT 01	340	6	15	0	37	0	0	117	1	0	8	2	0	0	1	0
WSDOT 02	128	19	31	0	1	0	0	8	0	0	2	2	0	0	2	0
WSDOT 03	71	99	59	0	1	1	0	30	0	3	1054	0	0	0	0	0
WSDOT 04	260	15	19	0	0	0	0	0	0	0	5	0	0	0	0	0
WSDOT 05	127	87	1	0	3	0	0	5	0	0	12	0	0	0	0	0
WSDOT 06	70	9	1	0	0	0	0	0	0	63	5	0	0	0	0	0

WSDOT 07	21	29	30	0	1	0	0	1	0	0	36	0	0	0	0	1
WSDOT 08	43	15	56	0	0	0	0	0	2	4	8	0	0	0	0	2
WSDOT 09	24	54	51	0	0	1	0	0	0	0	4	0	0	0	0	0
WSDOT 10	2	6	0	0	1	0	0	0	0	1	43	3	0	0	0	3
WSDOT 11	8	5	10	0	1	0	0	0	0	0	1	0	0	0	0	0
WSDOT 12	43	43	9	0	1	0	0	0	0	0	5	0	0	0	0	0
WSDOT 14	6	5	0	0	8	1	0	4	0	1	3	0	0	14	0	1
WSDOT 15	14	7	1	0	2	2	0	0	0	0	7	0	0	0	0	0
WSDOT 16	63	20	1	0	3	1	0	1	0	0	55	0	0	0	0	0
WSDOT 17	133	23	12	0	1	2	1	3	0	0	4	0	1	0	0	0
WSDOT 18	58	13	0	0	3	0	0	0	0	0	8	0	0	0	0	0
WSDOT 19	3	0	2	0	0	0	0	1	0	3	12	0	0	0	0	1
WSDOT 20	10	19	2	0	1	0	0	0	0	0	7	0	0	0	0	0
WSDOT 21	24	41	6	0	0	2	0	3	0	0	5	0	0	0	0	0
WSDOT 22	24	32	6	0	18	0	0	0	0	1	13	0	0	0	0	0
WSDOT 23	2	2	0	0	8	0	0	0	45	0	86	0	0	61	0	0
WSDOT 24	4	0	4	0	0	0	0	0	0	0	3	0	0	0	0	0
WSDOT 25	1	4	2	0	36	0	0	0	0	0	8	0	0	0	0	0
WSDOT 26	1	6	3	0	0	0	0	0	0	0	61	0	0	0	0	0
WSDOT 27	8	10	3	0	1	0	0	0	0	1	6	0	0	0	0	0
WSDOT 28	45	7	4	0	36	0	0	3	0	0	3	0	0	0	0	3
WSDOT 29	10	17	1	0	1	0	0	0	0	0	127	0	0	0	0	0
WSDOT 30	37	23	2	0	6	0	0	4	0	0	2	0	0	0	0	0

Page 50

Appendix B. Linear models using all deer (white-tailed and mule deer) combined to evaluate factors that influence abundance of deer-vehicle collisions (as represented by new carcasses on the road April 2017 – October 2017). The most parsimonious model provided evidence that abundance of deer-vehicle collisions was predicted best by $e^{(0.02397 + 0.09338*\text{predicted deer abundance} + 0.00008011*\text{minimum sight distance(ft)} - 0.00001301*\text{minimum sight distance(ft)}*\text{predicted deer abundance} + 0.05816*\text{max slope within 60 m (degrees)})}$. k = number of parameters, AICc = Akaike's Information Criterion, ΔAICc = difference in AICc between model and the most parsimonious model, AICc weight = relative model weight according to AICc (Burnham and Andeson 2002).

Model (predictors)	k	AICc	ΔAICc	AICc weight
Predicted deer abundance + minimum sight distance + predicted deer abundance*minimum sight distance + maximum slope within 60 m	5	162.7	0.00	0.33
Predicted deer abundance + maximum slope within 60 m	3	162.9	0.18	0.30
Predicted deer abundance + minimum sight distance + predicted deer abundance*minimum sight distance + maximum slope within 60 m + distance to building	6	164.5	1.77	0.13
Predicted mule deer abundance + minimum sight distance + predicted mule deer abundance*minimum sight distance	4	165.8	3.14	0.07
Minimum sight distance	2	165.9	3.27	0.06
Predicted deer abundance + minimum sight distance + predicted deer abundance*minimum sight distance + distance to building	4	167.4	4.47	0.03
Predicted deer abundance	2	167.4	4.71	0.03
Predicted deer abundance + minimum sight distance	3	168.2	5.54	0.02
Predicted deer abundance + distance to building	3	168.2	5.56	0.02

Appendix C. Posters and presentations presented at the Washington/Oregon Chapters of The Wildlife Society, Undergraduate Research Symposium at WSU Pullman Campus, and Mule Deer Summit at the Okanogan Trails Chapter of the Mule Deer Foundation.

Appendix D. This appendix was added to address post-report inquiries by Kaitlyn Maise, WSDOT. It summarizes a post hoc analysis to assess (1) the importance of deer abundance on deer-vehicle collisions and (2) the relative importance of various landscape factors as predictors of deer abundance. We included deer abundance in our original models of deer-vehicle collisions in Table 2 of the report because we presumed that the deer-vehicle collision process was a deer density-dependent process.

To assess the importance of deer abundance on deer-vehicle collisions, we expanded on the existing linear models and model selection procedures used in Table 2 of the report by adding 4 models to test for the importance of deer abundance on deer-vehicle collisions (Table D.1). In doing so, we tested for singular, additive, and interactive effects of deer abundance relative to the other factors listed. As in the original analysis, we found reasonable support (most parsimonious model with $\Delta AICc = 0$ and AICc weight = 0.59, with next best model having $\Delta AICc > 2.0$) for an interactive effect of deer abundance and minimum sight distance with an additive effect of maximum slope (Table D.1). The inclusion of the additional 4 models helped verify the importance of abundance, which had been included in our original analyses (Table 2).

To assess the relative importance of various landscape factors on deer abundance, we considered the same landscape metrics used in our initial analysis of frequency of deer crossings (Table 1) as predictors of deer abundance (Table D.2). We used the same linear modeling and model selection procedures used in the report. Two nested models emerged as competing, one with distance to open south-facing slope and the other with additive effects of distance to open south facing slope and distance to linear water feature (Table D.2). Based on the principle of parsimony and weight of evidence, we considered the simpler model with the effect of distance to open south facing slope as the most parsimonious of the two models ($\Delta AICc = 0.65$). In other words, there was little evidence that the addition of distance to linear water feature to this model helped improve the fit of the model to the data. The lack of importance of agriculture was surprising, but may be explained by the fact that the preponderance of data obtained and used here were from mule deer, which are generally considered browsers that forage on herbaceous and woody shrub vegetation relatively more than white-tailed deer, which are viewed more as grazers (Lyons et al. 2012). This may be further explained by habitat segregation between these two species, with mule deer being more typically distributed on surrounding slopes where they are more effective at evading predators compared to white-tailed deer in more gentle terrain (Lingle 2001, Lingle and Wilson 2001, Lingle 2002) where agriculture typically occurs.

Literature Cited

Lingle, S. 2001. Anti-predator strategies and grouping patterns in white-tailed deer and mule deer. Ethology 107, 295-314.
Lingle, S. and W.F. Wilson. 2001. Detection and avoidance of predators in white-tailed deer (*Odocoileus virginianus*) and mule deer (*O. hemionus*). Ethology 107, 125-147.
Lingle, S. 2002. Coyote predation and habitat segregation of white-tailed and mule deer. Ecology 2037-2048.
Lyons, R.K., T.D.A. Forbs, and R. Machen. 2012. What range herbivores eat – and why. Texas Agricultural Extension Service, Texas A&M University System, College Station. Report B-

6037. Available at: http://animalscience.tamu.edu/wp-content/uploads/sites/14/2012/04/B6037-rangeherbivores.pdf.

Table D.1. Linear models of deer-vehicle collision abundances (as represented by new carcasses on the road April 2017 – October 2017) between mile posts 176-201 of SR 20 in the Methow Valley, Washington, April – October 2017. This adds 4 models to Table 2 in the main report, to perform a post hoc analysis of the importance of deer abundance on the abundance of deer-vehicle collisions. See text for descriptions of predictors listed under model column. k = number of parameters, AICc = small sample corrected Akaike's Information Criterion, ΔAICc = difference in AICc between model and the most parsimonious model, AICc weight = relative model weight according to AICc.

Model (predictors)	k	AICc	ΔAICc	AICc weight
Predicted mule deer abundance + minimum sight distance + predicted mule deer abundance*minimum sight distance + maximum slope within 60 m	5	155.7	0.00	0.59
Predicted mule deer abundance + minimum sight distance + predicted mule deer abundance*minimum sight distance + maximum slope within 60 m + distance to building	6	158.0	2.3	0.19
Predicted mule deer abundance + minimum sight distance + predicted mule deer abundance*minimum sight distance	4	159.7	3.91	0.08
Predicted mule deer abundance + maximum slope within 60 m	3	161.1	5.33	0.04
Predicted mule deer abundance + minimum sight distance + predicted mule deer abundance*minimum sight distance + distance to building	4	161.6	5.88	0.03
Minimum sight distance + maximum slope within 60 m	3	162.8	7.01	0.02
Minimum sight distance + maximum slope within 60 m + distance to building	4	163.2	7.43	0.01
Predicted mule deer abundance + minimum sight distance + maximum slope within 60 m + distance to building	5	163.7	7.92	0.01
Predicted mule deer abundance + minimum sight distance	3	165.4	9.64	0.01
Predicted mule deer abundance	2	165.5	9.78	0.00
Minimum sight distance + distance to building	3	165.9	10.14	0.00
Minimum sight distance	2	165.9	10.21	0.00
Predicted mule deer abundance + distance to building	3	166.9	11.11	0.00

Table D.2. Linear models of estimated deer abundance between mile posts 176-201 of SR 20 in the Methow Valley, Washington, April-October 2017 and 2018. See text for details and descriptions of predictors listed under model column. k = number of parameters, AICc = small sample corrected Akaike's Information Criterion, ΔAICc = difference in AICc between model and the most parsimonious model, AICc weight = relative model weight according to AICc.

Model (predictors)	k	AICc	ΔAICc	AICc weight
Distance to open south-facing slope	2	174.5	0	0.65
Distance to open south-facing slope + distance to linear water feature	3	176.2	1.66	0.29
Distance to forest + distance to building + distance to agriculture + distance to linear water feature + distance to open south-facing slope	6	179.9	5.38	0.05
Distance to linear water feature	2	206.3	31.77	0.00
Distance to nearest building + distance to linear water feature	3	206.8	32.53	0.00
Distance to agriculture + distance to linear water feature	3	207.0	32.53	0.00
Distance to nearest forest patch + distance to linear water feature	3	208.4	33.89	0.00
Distance to agriculture	2	209.6	35.07	0.00
Distance to forest	2	211.4	36.91	0.00
Distance to building	2	212.3	37.77	0.00